Reprinted* From **Encyclopedia of Modern Optics**

Edited by Robert D. Guenther, Duncan G. Steel and Leopold Bayvel

Elsevier, Oxford, 2005

ISBN 0-12-227600-0

*(This version includes corrections of errors in the original text)

Free Electron Lasers

A Gover, Tel-Aviv University, Tel-Aviv, Israel

Introduction

The Free Electron Laser (FEL) is an exceptional kind of laser. Its active medium is not matter, but charged particles (electrons) accelerated to high energies, passing in vacuum through a periodic undulating magnetic field. This distinction is the main reason for the exceptional properties of FEL: operating at a wide range of wavelengths – from mm-wave to X-rays with tunability, high power, and high efficiency.

In this article we explain the physical principles of FEL operation, the underlying theory and technology of the device and various operating schemes, which have been developed to enhance performance of this device.

The term 'Free Electron Laser' was coined by John Madey in 1971, pointing out that the radiative transitions of the electrons in this device are between free space (more correctly – unbound) electron quantum states, which are therefore states of continuous energy. This is in contrast to conventional atomic and molecular lasers, in which the electron performs radiative transition between bound (and therefore of distinct energy) quantum states. Based on these theoretical observations, Madey and his colleagues in Stanford University demonstrated FEL operation first as an amplifier (at $\lambda = 10.6$ μm) in 1976, and subsequently as an oscillator (at $\lambda = 3.4$ μm) in 1980.

From the historical point of view, it turned out that Madey's invention was essentially an extension of a former invention in the field of microwave-tubes technology – the Ubitron. The Ubitron, a mm-wave electron tube amplifier based on a magnetic undulator, was invented and developed by Philips and Enderbry who operated it at high power levels in 1960. The early Ubitron development activity was not noticed by the FEL developers because of the disciplinary gap, and largely because its research was classified at the time. Renewed interest in high-power mm-wave radiation emission started in the 1970s, triggered by the development of pulsed-line generators of 'Intense Relativistic Beams' (IRB). This activity, led primarily by plasma physicists in the defense establishment laboratories of Russia (mostly IAP in Gorky – Nizhny Novgorod) and the US (mostly N.R.L. – DC) led to development of high-gain high-power mm-wave sources independently of the development of the optical FEL. The connection between these devices and between them to conventional microwave tubes (as Traveling Wave Tubes – TWT) and other electron beam radiation schemes, like Cenenkov and Smith-Purcell radiation that may also be considered FELs, was revealed in the mid-1970s, starting with the theoretical works of P. Spangle, A. Gover and A. Yariv who identified that all these devices satisfy the same dispersion equation as the TWT derived by John Pierce in the 1940s. Thus, the optical FEL could be conceived as a kind of immense electron tube, operating with a high-energy electron beam in the low gain regime of the Pierce TWT dispersion equation.

The extension of the low-gain FEL theory to the general 'electron-tube' theory is important because it led to development of new radiation schemes and new operating regimes of the optical FEL. This was exploited by physicists in the discipline of accelerator physics and synchrotron radiation, who identified, starting with the theoretical works of C. Pellegrini and R. Bonifacio in the early 1980s, that high-current, high-quality electron beams, attainable with further development of accelerators technology, could make it possible to operate FELs in the high-gain regime, even at short wavelengths (vacuum ultra-violet – VUV and soft X-ray), and that the high-gain FEL theory can be extended to include amplification of the incoherent synchrotron spontaneous emission (shot noise) emitted by the electrons in the undulator. These led to the important development of the 'self (synchrotron) amplified spontaneous emission (SASE) FEL', which promised to be an extremely high brightness radiation source, overcoming the fundamental obstacles of X-ray lasers development: lack of mirrors (for oscillators) and lack of high brightness radiation sources (for amplifiers).

A big boost to the development of FEL technology was given during the period of the American 'strategic defense initiative – SDI' (Star-Wars) program in the mid-1980s. The FEL was considered one of the main candidates for use in a ground-based or space-based 'directed energy weapon – DEW', that can deliver megawatts of optical power to hit attacking missiles. The program led to heavy involvement of major American defense establishment laboratories (Lawrence–Livermore National Lab, Los-Alamos National Lab) and contracting companies (TRW, Boeing). Some of the outstanding results of this effort were demonstration of the high-gain operation of an FEL amplifier in the mm-wavelength regime, utilizing an Induction Linac (Livermore, 1985), and demonstration of enhanced radiative energy extraction efficiency in FEL oscillator, using a 'tapered wiggler' in an RF-Linac driven FEL oscillator (Los-Alamos, 1983). The program has not been successful in demonstrating the potential of FELs to operate at the high average power levels needed for DEW applications. But after the cold-war period, a small part of the program continues to support research and development of medical FEL application.

Principles of FEL Operation

Figure 1 displays schematically an FEL oscillator. It is composed of three main parts: an electron accelerator, a magnetic wiggler (or undulator), and an optical resonator.

Without the mirrors, the system is simply a synchrotron undulator radiation source. The electrons in the injected beam oscillate transversely to their propagation direction z, because of the transverse magnetic Lorenz force:

$$\mathbf{F}_\perp = -ev_z\hat{\mathbf{e}}_z \times \mathbf{B}_\perp \qquad [1]$$

In a planar (linear) wiggler, the magnetic field on axis is approximately sinusoidal:

$$\mathbf{B}_\perp = B_w\hat{e}_y \cos k_w z. \qquad [2]$$

In a helical wiggler:

$$\mathbf{B}_\perp = B_w(\hat{\mathbf{e}}_y \cos k_w z + \hat{\mathbf{e}}_x \sin k_w z) \qquad [3]$$

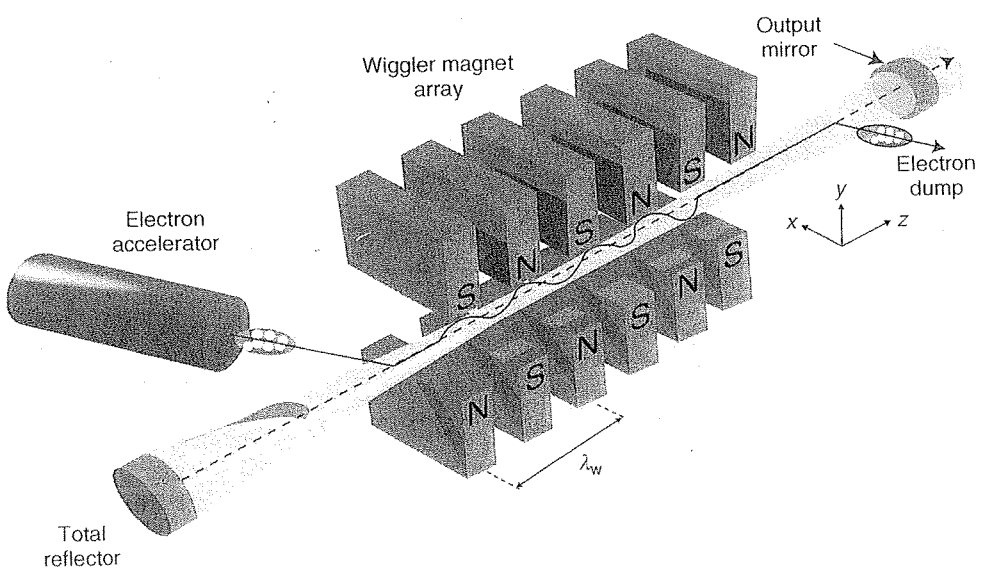

Figure 1 Components of a FEL-oscillator. (Reproduced from Benson SV (2003) Free electron lasers push into new frontiers. *Optics and Photonics News* 14: 20–25. Illustration by Jaynie Martz.)

In either case, if we assume constant (for the planar wiggler – only on the average) axial velocity, then $z = v_z t$. The frequency of the transverse force and the mechanical oscillation of the electrons, as viewed transversely in the laboratory frame of reference, is:

$$\omega_{0s} = k_w v_z = 2\pi \frac{v_z}{\lambda_w} \qquad [4]$$

where $\lambda_w = 2\pi/k_w$ is the wiggler period.

The oscillating charge emits an electromagentic radiation wavepacket. In a reference frame moving with the electrons, the angular radiation pattern looks exactly like dipole radiation, monochromatic in all directions (except for the frequency-line-broadening due to the finite oscillation time, i.e., the wiggler transit time). In the laboratory reference-frame the radiation pattern concentrates in the propagation ($+z$) direction, and the Doppler up-shifted radiation frequency depends on the observation angle Θ relative to the z-axis:

$$\omega_0 = \frac{\omega_{0s}}{1 - \beta_z \cos \Theta} \qquad [5]$$

On axis ($\Theta = 0$), the radiation frequency is:

$$\omega_0 = \frac{ck_w\beta_z}{1 - \beta_z} = (1 + \beta_z)\beta_z\gamma_z^2 ck_w \cong 2\gamma_z^2 ck_w \qquad [6]$$

where $\beta_z \equiv v_z/c$, $\gamma_z \equiv (1 - \beta_z^2)^{-1/2}$ are the axial (average) velocity and the axial Lorenz factor, respectively, and the last part of the equation is valid only in the (common) highly relativistic limit $\gamma_z \gg 1$.

Using the relations $\beta_z^2 + \beta_\perp^2 = \beta^2$, $\beta_\perp = a_w/\gamma$, one can express γ_z:

$$\gamma_z = \frac{\gamma}{1 + a_w^2/2} \qquad [7]$$

(this is for a linear wiggler, as well as a helical wiggler; for both definitions (2,3)$\langle B_\perp^2(z)\rangle = B_w^2/2$).

$$\gamma \equiv (1 - \beta^2)^{-1/2} = 1 + \frac{\varepsilon_k}{mc^2}$$
$$= 1 + \varepsilon_k\,[\mathrm{MeV}]/0.511 \qquad [8]$$

and a_w – (also termed K) 'the wiggler parameter' is the normalized transverse momentum:

$$a_w = \frac{eB_w}{k_w mc} = 0.093 B_w\,[\mathrm{KGauss}]\lambda_w\,[\mathrm{cm}] \qquad [9]$$

Typical values of B_w in FEL wigglers (undulators) are of the order of Kgauss', and λ_w of the order of CMs, and consequently $a_w < 1$. Considering that electron beam accelerator energies are in the range of MeV to GeV, one can appreciate from eqns [6]–[8], that a significant relativistic Doppler shift factor $2\gamma_z^2$, in the range of tens to millions, is possible. It, therefore, provides incoherent synchrotron undulator radiation in the frequency range of microwave to hard X-rays.

Synchrotron undulator radiation was studied in 1951 and since then has been a common source of VUV radiation in synchrotron facilities. From the point of view of laser physics theory, this radiation can be viewed as 'spontaneous synchrotron radiation emission' in analogy to spontaneous radiation emission by electrons excited to higher bound-electron quantum levels in atoms or molecules. Alternatively, it can be regarded as the classical shot noise radiation, associated with the current fluctuations of the randomly injected discrete charges comprising the electron beam. Evidently this radiation is incoherent, and the fields it produces average in time to zero, because the wavepackets emitted by the randomly injected electrons interfere at the observation point with random phase. However, their energies sum up and can produce substantial power.

Based on fundamental quantum-electrodynamical principles or Einstein's relations, one would expect that any spontaneous emission scheme can be stimulated. This principle lies behind the concept of the FEL, which is nothing but stimulated undulator synchrotron radiation. By stimulating the electron beam to emit radiation, it is possible, as with any laser, to generate a coherent radiation wave and extract more power from the gain medium, which in this case is an electron beam, that carries an immense amount of power. There are two kinds of laser schemes which utilize stimulation of synchrotron undulator radiation:

(i) *A laser amplifier.* In this case the mirrors in the schematic configuration of **Figure 1** are not present, and an external radiation wave at frequencies within the emission range of the undulator is injected at the wiggler entrance. This requires, of course, an appropriate radiation source to be amplified and availability of sufficiently high gain in the FEL amplifier.

(ii) *A laser oscillator.* In this case an open cavity (as shown in **Figure 1**) or another (waveguide) cavity is included in the FEL configuration. As in any laser, the FEL oscillator starts building up its radiation from the spontaneous (synchrotron undulator) radiation which gets trapped in the resonator and amplified by stimulated emission along the wiggler. If the threshold condition is satisfied (having single path gain higher than the round trip losses), the oscillator arrives to saturation and steady state coherent operation after a short transient period of oscillation build-up.

Because the FEL can operate as a high-gain amplifier (with a long enough wiggler and an electron beam of high current and high quality), also a third mode of operation exists: self amplified spontaneous emission (SASE). In this case, the resonator mirrors in Figure 1 are not present and the undulator radiation generated spontaneously in the first sections of the long undulator is amplified along the wiggler and emitted at the wiggler exit at high power and high spatial coherence.

The Quantum-Theory Picture

A free electron, propagating in unlimited free space, can never emit a single photon. This can be proven by examining the conservation of energy and momentum conditions:

$$\varepsilon_{k_i} - \varepsilon_{k_f} = \hbar\omega \qquad [10]$$

$$\mathrm{k_i} - \mathrm{k_f} = \mathrm{q} \qquad [11]$$

that must be satisfied, when an electron in an initial free-space energy and momentum state $(\varepsilon_{k_i}, \hbar k_i)$ makes a transition to a final state $(\varepsilon_{k_f}, \hbar k_f)$, emitting a single photon of energy and momentum $(\hbar\omega, \hbar q)$. In free space:

$$\varepsilon_k = c\sqrt{(\hbar \mathrm{k})^2 + (mc^2)^2} \qquad [12]$$

$$\mathrm{q} = \frac{\omega}{\mathrm{c}}\hat{\mathrm{e}}_q \qquad [13]$$

and eqns [10]–[13] have only one solution, $\omega = 0$, $\mathrm{q} = 0$. This observation is illustrated graphically in the energy–momentum diagram of Figure 2a in the framework of a one-dimensional model. It appears that if both eqns [10] and [11] can be satisfied, then the phase velocity of the emitted radiation wave $v_{\mathrm{ph}} = \omega/q$ (the slope of the chord) will equal the electron wavepacket group velocity $v_{\mathrm{g}} = v_z$ at some intermediate point $k^* = p^*/\hbar$:

$$v_{\mathrm{ph}} = \frac{\omega}{q} = \frac{\varepsilon_{ki} - \varepsilon_{kf}}{\hbar(k_i - k_f)} = \left.\frac{\partial\varepsilon}{\partial p}\right|_{p^*} = v_{\mathrm{g}} \qquad [14]$$

For a radiation wave in free space (eqn [13]), this results in $c = v_{\mathrm{g}}$, which contradicts special relativity.

The reason for the failure to conserve both energy and momentum in the transition is that the photon momentum $\hbar q$ it too small to absorb the large momentum shift of the electron, as it recoils while releasing radiative energy $\hbar\omega$. This observation leads to ideas on how to make a radiative transition possible:

(i) *Limit the interaction length.* If the interaction length is L, the momentum conservation

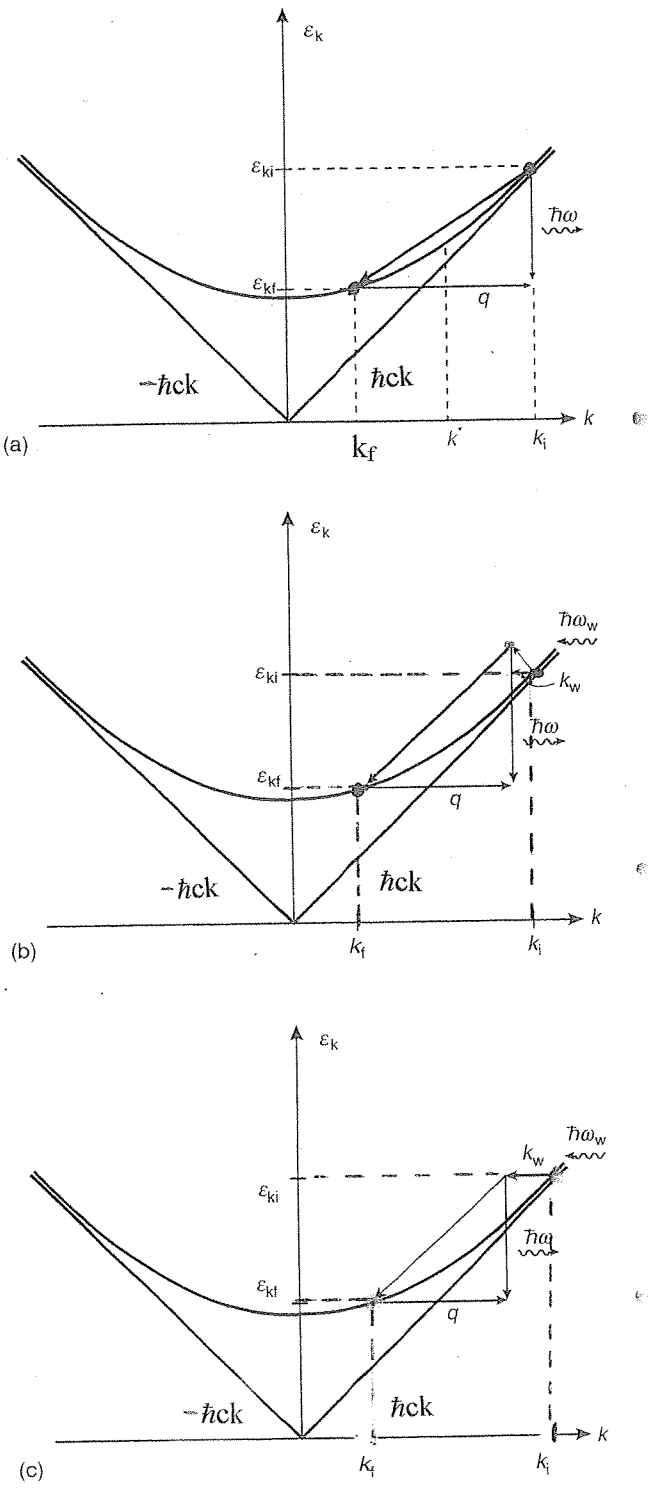

Figure 2 Conservation of energy and momentum in forward photon emission of a free electron: (a) The slope of the tangent to the curve at intermediate point k^*, $\partial\varepsilon_k(k^*)/\partial k$ may be equal to the slope of the chord $\hbar\omega/q$ which is impossible in free space. (b) electron radiative transition made possible with an electromagnetic pump (Compton Scattering). (c) The wiggler wavenumber – k_w conserves the momentum in electron radiative transition of FEL.

condition in eqn [11] must be satisfied only within an uncertainty range $\pm\pi/L$. This makes it possible to obtain radiative emission in free electron radiation effects like 'Transition Radiation' and in microwave tubes like the Klystron.

(ii) *Propagate the radiation wave* in a 'slow wave' structure, where the phase velocity of the radiation wave is smaller than the speed of light, and satisfaction of eqn [14] is possible. For example, in the Cerenkov effect, charged particles pass through a medium (gas) with index of refraction $n > 1$. Instead of eqn [13], $\mathrm{q} = n(\omega)(\omega/c)\hat{\mathrm{e}}_q$, and consequently $q_z = n(\omega)(\omega/c)\cos\Theta_q$, where we assume radiative emission at an angle Θ_q relative to the electron propagation axis z. Substitution in eqn [14] results in the Cerenkov radiation condition $v_g n(\omega)\cos\Theta_q = 1$.

Another example for radiation emission in a slow-wave structure is the Traveling Wave Tube (TWT). In this device, a periodic waveguide of periodicity λ_w permits (via the Floquet theorem) propagation of slow partial waves (space harmonics) with increased wavenumber $q_z + mk_w$ ($m = 1, 2, \ldots$), and again eqn [14] can be satisfied.

(iii) *Rely on a 'two-photon' radiative transition.* This can be 'real photon' Compton scattering of an intense radiation beam (electromagnetic pump) off an electron beam, or 'virtual photon' scattering of a static potential, as is the case in bremsstrahlung radiation and in synchrotron–undulator radiation. The latter radiation scheme may be considered as a 'magnetic brehmsstrahlung' effect or as 'zero frequency pump' Compton scattering, in which the wiggler contributes only 'crystal momentum' $\hbar k_w$, to help satisfy the momentum conservation condition in eqn [11]. The Compton scattering scheme is described schematically for the one-dimensional (back scattering) case in **Figure 3**, and its conservation of energy and momentum diagram is depicted in **Figure 2b** (a 'real photon' (ω_w, k_w) free-space pump wave is assumed with $k_w = \omega_w/c$). The analogous diagram of a static wiggler ($\omega_w = 0$, $k_w = 2\pi/\lambda_w$) is shown in **Figure 2c**. It is worth noting that the effect of the incident scattered wave or the wiggler is not necessarily a small perturbation. It may modify substantially the electron energy-dispersion diagram of the free electron and a more complete 'Brillouin diagram' should be used in **Figure 2c**. In this sense, the wiggler may be viewed as the analogue of a one-dimensional crystal, and its period λ_w analogous to the crystal lattice constant. The momentum conservation during a radiation transition, with the aid of the wiggler 'crystal momentum' $\hbar k_w$ is quite analogous to the occurrence of vertical radiative transitions in direct bandgap semiconductors, and thus the FEL has, curiously enough, some analogy to microscopic semiconductor lasers.

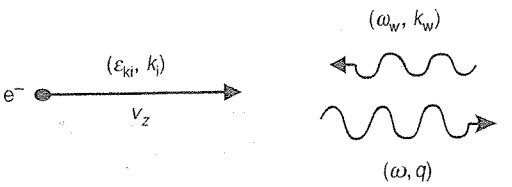

Figure 3 The scheme of backward scattering of an electromagnetic wave off an electron beam (Doppler shifted Compton scattering).

All the e-beam radiation schemes already mentioned can be turned into stimulated emission devices, and thus may be termed 'free electron lasers' in the wide sense. The theory of all of these devices is closely related, but most of the technological development was carried out on undulator radiation (Magnetic brehmsstrahlung) FELs, and the term FEL is usually reserved for this kind (though some developments of Cerenkov and Smith–Purcell FELs are still carried out).

When considering a stimulated emission device, namely enhanced generation of radiation in the presence of an external input radiation wave, one should be aware, that in addition to the emission process described by eqns [10] and [11] and made possible by one of the radiation schemes described above, there is also a stimulated absorption process. Also, this electronic transition process is governed by the conservation of energy and momentum conditions, and is described by eqns [10] and [11] with k_i and k_f exchanged.

Focusing on undulator-radiation FEL and assuming momentum conservation in the axial (z) dimension by means of the wiggler wavenumber k_w, the emission and absorption quantum transition levels and radiation frequencies are found from the solution of equations:

$$\varepsilon_{k_{zi}} - \varepsilon_{k_{zf}} = \hbar\omega_e \qquad [15a]$$

$$k_{zi} - k_{zf} = q_{ze} + k_w \qquad [15b]$$

$$\varepsilon_{k_{za}} - \varepsilon_{k_{zi}} = \hbar\omega_a \qquad [16a]$$

$$k_{za} - k_{zi} = q_{za} + k_w \qquad [16b]$$

For fixed k_w, fixed transverse momentum and given e-beam energy $\varepsilon_{k_{zi}}$ and radiation emission angle Θ_q ($q_z = (\omega/c)\cos\Theta_q$), eqns [15] and [16] have separately

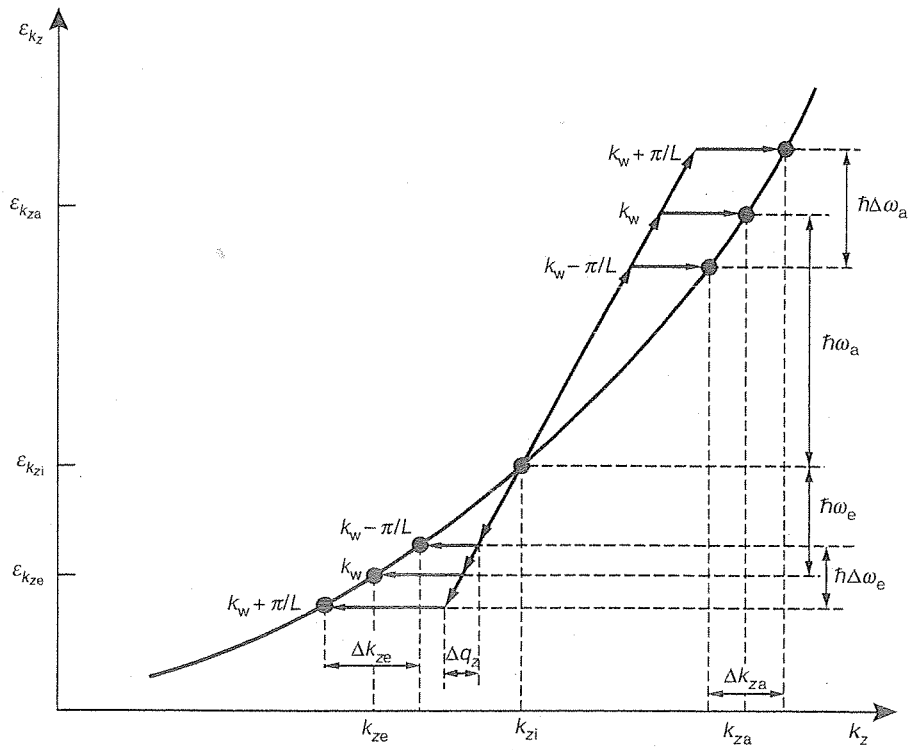

Figure 4 The figure illustrates that the origin of difference between the emission and absorption frequencies is the curvature of the energy dispersion line, and the origin of the homogeneous line broadening is momentum conservation uncertainty $\pm\pi/L$ in a finite interaction length. (Reproduced with permission from Friedman A, Gover A, Ruschin S, Kurizki G and Yariv A (1988) Spontaneous and stimulated emission from quasi-free electrons. *Reviews of Modern Physics* 60: 471–535. Copyright (1988) by the American Physical Society.)

distinct solutions, defining the electron upper and lower quantum levels for radiative emission and absorption respectively. The graphical solutions of these two set of equations are shown in **Figure 4**, which depicts also the 'homogeneous' frequency-line broadening $\hbar\Delta\omega_e$, $\hbar\Delta\omega_a$ of the emission and absorption lines due to the uncertainty in the momentum conservation $\pm\pi/L$ in a finite interaction length. In the quantum limit of a cold (monoenergetic) e-beam and a long interaction length L, the absorption line center ω_a is larger than the emission line center ω_e, and the linewidths $\Delta\omega_e \cong \Delta\omega_a = \Delta\omega_L$ are narrower than the emission and absorption lines spacing $\omega_a - \omega_e$, as shown in **Figure 5a**. The FEL then behaves as a 3-level quantum system, with electrons occupying only the central level, and the upper level is spaced apart from it more than the lower level (**Figure 4**).

In the classical limit $\hbar \to 0$, one can Taylor-expand ε_{kz} around k_{zi}. Using:

$$v_z = \frac{1}{\hbar}\frac{\partial\varepsilon_{kz}}{\partial k_z}, \qquad \frac{1}{\gamma_z^2\gamma m} = \frac{1}{\hbar^2}\frac{\partial^2\varepsilon_{kz}}{\partial k_z^2}$$

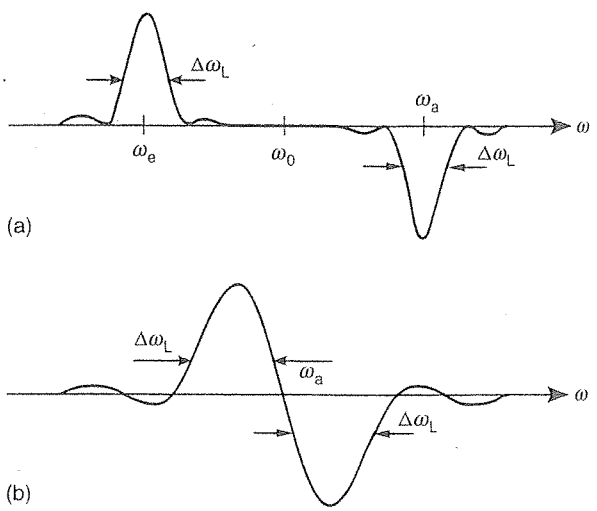

Figure 5 Net gain emission/absorption frequency lines of FEL: (a) in the quantum limit: $\omega_a - \omega_e \gg \Delta\omega_L$, (b) in the classical limit: $\omega_a - \omega_e \ll \Delta\omega_L$.

one obtains:

$$\omega_e \cong \omega_a \cong \omega_0 = v_z(q_{z0} + k_w) \qquad [17]$$

which for $q_{z0} = (\omega/c)\cos\Theta_q$ reproduces the classical synchronism condition in eqn [5]. The homogeneous

broadening linewidth is found to be:

$$\frac{\Delta\omega_L}{\omega_0} = \frac{1}{N_w} \qquad [18]$$

where $N_w = L/\lambda_w$ is the number of wiggler periods.

The classical limit condition requires that the difference between the emission and absorption line centers will be smaller than their width. This is expressed in terms of the 'recoil parameter' ε' (for $\Theta_q = 0$):

$$\varepsilon = \frac{\omega_a - \omega_e}{\Delta\omega_L} = \frac{1+\beta}{\beta_z^2}\frac{\hbar\omega_0}{\gamma mc^2}N_w \ll 1 \qquad [19]$$

This condition is satisfied in all practical cases of realizable FELs. When this happens, the homogeneous line broadening dominates over the quantum-recoil effect, and the emission and absorption lines are nearly degenerate (**Figure 5b**). The total quantum-electrodynamic photonic emission rate expression:

$$\frac{dv_q}{dt} = \Gamma_{sp}[(v_q+1)F(\omega-\omega_e) - v_qF(\omega-\omega_a)] \qquad [20]$$

reduces then into:

$$\frac{dv_q}{dt} = v_q\Gamma_{sp}\varepsilon\Delta\omega_L\frac{d}{d\omega}F(\omega-\omega_e) + \Gamma_{sp}F(\omega-\omega_0) \qquad [21]$$

Here v_q is the number of photons in radiation mode q, Γ_{sp} – the spontaneous emission rate, and $F(\omega-\omega_0)$ is the emission (absorption) lineshape function. **Figure 5b** depicts the transition of the net radiative emission/absorption rate into a gain curve which is proportional to the derivative of the spontaneous emission lineshape function (first term in eqn [21]). Equation [21] presents a fundamental relation between the spontaneous and stimulated emission of FELs, which was observed first by John Madey (Madey's theorem). It can be viewed as an extension of Einstein's relations to a classical radiation source.

The Classical Picture

The spontaneous emission process of FEL (synchrotron undulator radiation) is nothing but dipole radiation of the undulating electrons, which in the laboratory frame of reference is Doppler shifted to high frequency. The understanding of the stimulated emission process requires a different approach.

Consider a single electron, following a sinusoidal trajectory under the effect of a planar undulator magnetic field in eqn [2] (**Figure 1**):

$$v_x = v_w\cos k_w z_e(t) \qquad [22]$$

$$x = x_w\sin k_w z_e(t) \qquad [23]$$

where $v_w = ca_w/\gamma$ and $x_w = v_w/(v_z k_w)$. An electromagnetic wave $E_x(z,t) = E_0\cos(\omega t - k_z z)$ propagates collinearly with the electron. **Figure 6** displays the electron and wave 'snap-shot' positions as they propagate along one wiggler period λ_w.

If the electron, moving at average axial velocity v_z, enters the interaction region $z = 0$ at $t = 0$, its axial position is $z_e(t) = v_z t$, and the electric force it experiences is $-eE_x(z_e(t),t) = -eE_0\cos(\omega - k_z v_z)t$. Clearly, this force is (at least initially at $t = 0$) opposite to the transverse velocity of the electron $v_x = v_w\cos(k_w v_z)t$ (imply in deceleration) and the power exchange rate $-ev_e\cdot E = -ev_xE_x$ corresponds to transfer of energy into the radiation field on account of the electron kinetic energy. Because the phase velocity of the radiation mode is larger than the electron velocity, $v_{ph} = \omega/k_z > v_z$, the electron phase $\varphi_e = (\omega - k_z v_z)t$ grows, and the power exchange rate $-ev_xE_x$ changes. However, if one synchronizes the electron velocity, so that while the electron traverses one wiggler period ($t = \lambda_w/v_z$), the electron phase advances by 2π: $(\omega - k_z v_z)\cdot\lambda_w/v_z = 2\pi$, then the power exchange rate from the electron to the wave remains non-negative through the entire interaction length, because then the electron transverse velocity

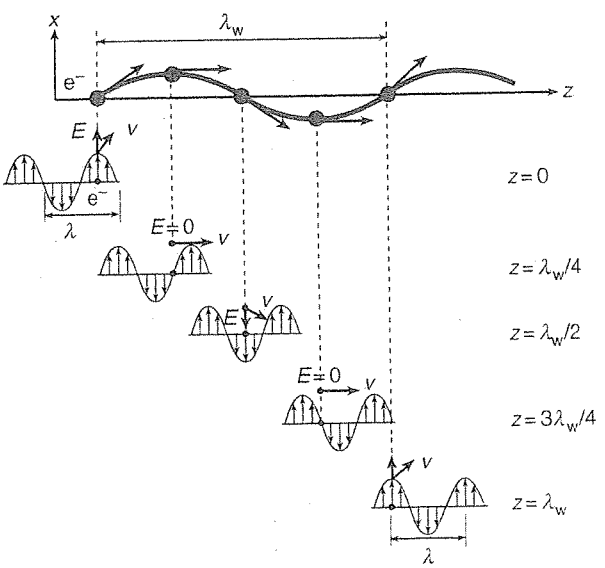

Figure 6 'Snapshots' of an electromagnetic wave period slipping relative to an undulating electron along one wiggler period λ_w. The energy transfer to the wave – $ev\cdot E$ remains non-negative all along.

v_x and the wave electric field E_x reverse sign, at each period exactly at the same points ($\lambda_w/4, 3\lambda_w/4$). This situation is depicted in **Figure 6**, which shows the slippage of the wave crests relative to the electron at five points along one wiggler period. The figure describes the synchronism condition, in which the radiation wave slips one optical period ahead of the electron, while the electron goes through one wiggle motion. In all positions along this period, $v \cdot E \geq 0$ (in a helical wiggler and a circularly polarized wave this product is constant and positive $v \cdot E > 0$ along the entire period). Substituting $\lambda_w = 2\pi/k_w$, this phase synchronism condition may be written as:

$$\frac{\omega}{v_z} = k_z + k_w \qquad [24]$$

which is the same as eqns [17] and [5].

Figure 6 shows that a single electron (or a bunch of electrons of duration smaller than an optical period) would amplify a co-propagating radiation wave, along the entire wiggler, if it satisfies the synchronism condition in eqn [24] and enters the interaction region ($z = 0$) at the right (decelerating) phase relative to the radiation field. If the electron enters at the opposite phase it accelerates (on account of the radiation field energy which is then attenuated by 'stimulated absorption'). Thus, when an electron beam is injected into a wiggler at the synchronism condition with electrons entering at random times, no net amplification or absorption of the wave is expected on the averages. Hence, some more elaboration is required, in order to understand how stimulated emission gain is possible then.

Before proceeding, it is useful to define the 'pondermotive force' wave. This force originates from the nonlinearity of the Lorenz force equation:

$$\frac{d}{dt}(\gamma m \mathbf{v}) = -e(\mathbf{E} + \mathbf{v} \times \mathbf{B}) \qquad [25]$$

At zero order (in terms of the radiation fields), the only field force on the right-hand side of eqn [25] is due to the strong wiggler field (eqns [2] and [3]), which results in the transverse wiggling velocity (eqn [22] for a linear wiggler). When solving next eqn [25] to first order in terms of the radiation fields:

$$\begin{aligned} E_s(r, t) &= \mathrm{Re}[\tilde{E}_s\, e^{i(k_z z - \omega t)}] \\ B_s(r, t) &= \mathrm{Re}[\tilde{B}_s\, e^{i(k_z z - \omega t)}] \end{aligned} \qquad [26]$$

the cross product $\mathbf{v} \times \mathbf{B}$ between the transverse components of the velocity and the magnetic field generates a longitudinal force component:

$$F_{pm}(z, t) = \mathrm{Re}[\hat{e}_z \tilde{F}_{pm} e^{i(k_z + k_w)z - i\omega t}] \qquad [27]$$

that varies with the beat wavenumber $k_s + k_w$ at slow phase velocity ($v_{ph} = \omega/(k_z + k_w) < c$). This slow force-wave is called the pomdermotive (PM) wave. Assuming the signal radiation wave in eqn [26] is polarization-matched to the wiggler (linearly polarized or circularly polarized for a linear or helical wiggler respectively), the PM force amplitude is given by:

$$|\tilde{F}_{pm}| = e|\tilde{E}_{s\perp}|a_w/2\gamma\beta_z \qquad [28]$$

With large enough k_w, it is always possible to slow down the phase velocity of the pondermotive wave until it is synchronized with the electron velocity:

$$v_{ph} = \frac{\omega}{k_z + k_w} = v_z \qquad [29]$$

and can apply along the interaction length a decelerating axial force, that will cause properly phased electrons to transfer energy to the wave on account of their longitudinal kinetic energy.

This observation is of great importance. It reveals that even though the main components of the wiggler and radiation fields are transverse, the interaction is basically longitudinal. This puts the FEL on an equal footing with the slow-wave structure devices as the TWT and the Cerenkov–Smith–Purcell FELs, in which the longitudinal interaction takes place with the longitudinal electric field component of a slow TM radiation mode. The synchronism condition in eqn [29] between the pondermotive wave and the electron, which is identical with the phase-matching condition in eqn [24], is also similar to the synchronism condition between an electron and a slow electromagnetic wave (eqn [14]).

Using the pondermotive wave concept, we can now explain the achievement of gain in the FEL with a random electron beam. **Figure 7** illustrates the interaction between the pondermotive wave and electrons, distributed at the entrance ($z = 0$) randomly within the wave period. **Figure 7a** shows 'snap-shots' of the electrons in one period of the pondermotive wave $\lambda_{pm} = 2\pi/(k_z + k_w)$ at different points along the wiggler, when it is assumed that the electron beam is perfectly synchronous with the pondermotive wave $v_{ph} = v_0$. As explained before, some electrons are slowed down, acquiring negative velocity increment Δv. However, for each such electron, there is another one, entering the wiggler at an accelerating phase of the wave, acquiring the same positive velocity increment Δv. There is then no net change in the energy of the e-beam or the wave, however, there is clearly an effect of 'velocity-bunching' (modulation), which turns along the wiggler into 'density-bunching' at the same

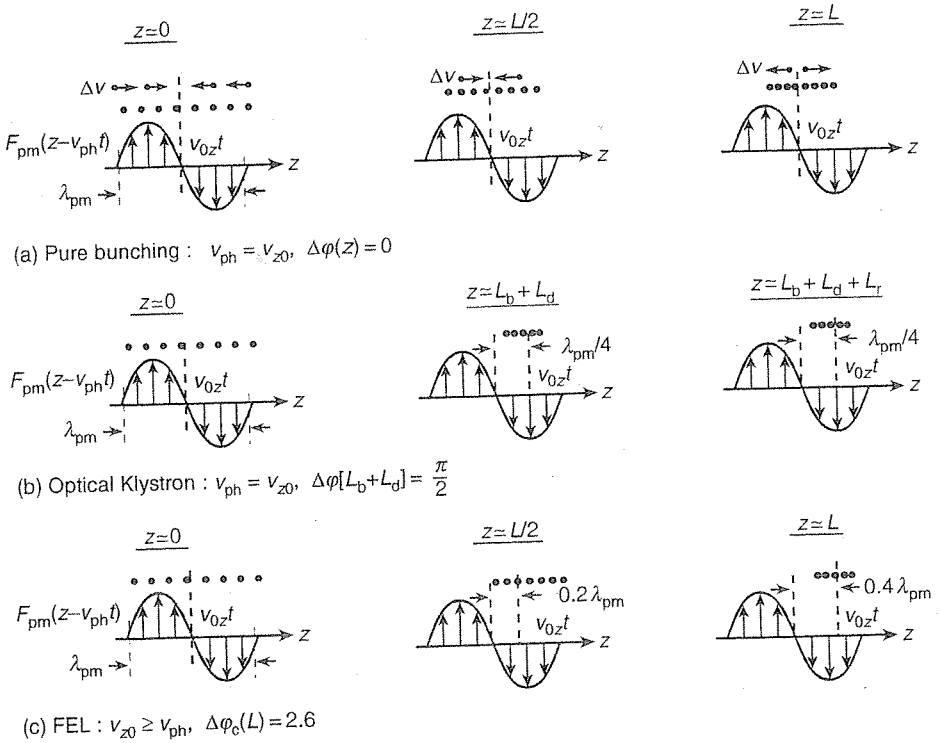

Figure 7 'Snapshots' of a pondermotive wave period, interacting along the interaction length L with an initially uniformly-distributed electron beam: (a) Pure bunching at exact synchronism in a uniform wiggler. (b) Energy bunching, density bunching and radiative emission taking place, respectively, in the energy buncher ($0 < z < L_b$), dispersive magnet ($L_b < z < L_b + L_d$) and radiating wiggler ($L_b + L_d < z < L_b + L_d + L_r$) sections of an Optical-Klystron. (c) Slippage from bunching phase to radiating phase at optimum detuning condition off synchronism in a uniform wiggler FEL.

frequency ω and wavenumber $k_z + k_w$ as the modulating pondermotive wave. The degree of density-bunching depends on the amplitude of the wave and the interaction length L. In the nonlinear limit the counter propagating (in the beam reference frame) velocity modulated electrons may over-bunch, namely cross over, and debunch again.

Bunching is the principle of classical stimulated emission in electron beam radiation devices. If the e-beam had been prebunched in the first place, we would have injected it at a decelerating phase relative to the wave and obtained net radiation gain right away (super radiant emission). This is indeed the principle behind the 'Optical-Klystron' (OK) demonstrated in **Figure 7b**. The structure of the OK is described ahead in **Figure 19**. The electron beam is velocity (energy) modulated by an input electromagnetic radiation wave in the first 'bunching-wiggler section' of length L_b. It then passes through a drift-free 'energy-dispersive magnet section' (chicane) of length L_d, in which the velocity modulation turns into density bunching. The bunched electron beam is then injected back into a second 'radiating-wiggler section', where it co-propagates with the same electromagnetic wave but with a phase advance of $\pi/2 - m2\pi$, $m = 1, 2, \ldots$ (spatial lag of $\lambda_{pm}/4 - m\lambda_{pm}$ in real space) which places the entire bunch at a decelerating phase relative to the PM-wave and so amplifies the radiation wave.

The principle of stimulated-emission gain in FEL, illustrated in **Figure 7c**, is quite similar. Here the wiggler is uniform along the entire length L, and the displacement of the electron bunches into a decelerating phase position relative to the PM-wave is obtained by injecting the electron beam at a velocity v_{z0}, slightly higher than the wave v_{ph} (velocity detuning). The detailed calculation shows that detuning corresponding to a phase shift of $\Delta\Psi(L) = [(\omega/v_{z0}) - (k_z + k_w)]L = -2.6$ (corresponding to spatial bunch advance of $0.4\lambda_{pm}$ along the wiggler length), provides sufficient synchronism with the PM-wave in the first half of the wiggler to obtain bunching, and sufficient deceleration-phasing of the created bunches in the second part of the wiggler to obtain maximum gain.

Principles of FEL Theory

The 3D radiation field in the interaction region can be expanded in general in terms of a complete set of

free-space or waveguide modes $\{\varepsilon_q(x,y), \mathcal{H}_q(x,y)\}$:

$$E(r,t) = \mathrm{Re}\Big[\sum_q c_q(z)\varepsilon_q(x,y)e^{i(k_{zq}z-\omega t)}\Big] \qquad [30]$$

The mode amplitudes $C_q(z)$ may grow along the wiggler interaction length $0 < z < L$, according to the mode excitation equation:

$$\frac{d}{dz}C_q(z) = -\frac{1}{4\mathcal{P}}e^{-ik_{zq}z}\int\int \tilde{\mathbf{J}}(x,y,z)\cdot\varepsilon_q^*(x,y)\,dx\,dy \qquad [31]$$

where $\mathcal{P} = -\frac{1}{2}\mathrm{Re}\int\int \varepsilon_q \times \mathcal{H}_q^* \cdot \hat{e}_z\,dx\,dy$ is the mode normalization power, and $\tilde{J}$ is the bunching current component at frequency ω, that is phase matched to the radiation waves, and needs to be calculated consistently from the electron force equations.

The FEL Small Signal Regime

We first present the basic formulation of FEL gain in the linear (small signal) regime, namely the amplified radiation field is assumed to be proportional to the input signal radiation field, and the beam energy loss is negligible. This is done in the framework of a one-dimensional (single transverse radiation mode) model.

The electron beam charge density, current density, and velocity modulation are solved in the framework of a one-dimensional plasma equations model (kinetic or fluid equations). The longitudinal PM-force in eqn [27] modulates the electron beam velocity via the longitudinal part of the force eqn [25]. This brings about charge modulation $\rho(z,t) = \mathrm{Re}[\tilde{\rho}(k_z + k_w, \omega)e^{i(k_z+k_w)z-i\omega t}]$ and consequently, also longitudinal space-charge field $\tilde{E}_{sc}(k_{zq} + k_w, \omega)$ and longitudinal current density modulation $\tilde{J}_z(k_z + k_w, \omega)$, related through the Poison and continuity equations:

$$i(k_z + k_w)\tilde{E}_{sc}(k_z + k_w, \omega) = \tilde{\rho}(k_z + k_w, \omega)/\varepsilon \qquad [32]$$

$$(k_z + k_w)\tilde{J}_z(k_z + k_w, \omega) = \omega\tilde{\rho}(k_z + k_w, \omega) \qquad [33]$$

Solving the force eqn [25] for a general longitudinal force $F_z(z,t) = \mathrm{Re}[\tilde{F}_z(k_z,\omega)e^{i(k_z z-\omega t)}]$ results in a linear longitudinal current response relation:

$$\tilde{J}_z(k_z,\omega) = -i\omega\chi_p(k_z,\omega)\tilde{F}_z(k_z,\omega)/(-e) \qquad [34]$$

where $\chi_p(k_z, \omega)$ is the longitudinal susceptibility of the electron beam 'plasma'.The beam charge density in the FEL may be quite high, and consequently the space charge field $\tilde{E}_{sc}$, arising from the Poison eqn [32], may not be negligible. One should take into consideration then that the total longitudinal force $\tilde{F}_z$ is composed of both the PM-force of eqn [27] and an arising longitudinal space-charge electric force $-e\tilde{E}_{sc}$.

Thus, one should substitute in eqn [34]:

$$\tilde{F}_z(k_z + k_w, \omega) = -e\left[\tilde{E}_{pm}(k_z + k_w, \omega) + \tilde{E}_{sc}(k_z + k_w, \omega)\right] \qquad [35]$$

and solve it self-consistently with eqns [32] and [33] to obtain the 'external-force' response relation:

$$\tilde{J}_z(k_z + k_w, \omega) = \frac{-i\omega\chi_p(k_z + k_w, \omega)}{1 + \chi_p(k_z + k_w, \omega)/\varepsilon}\tilde{E}_{pm}(k_z + k_w, \omega) \qquad [36]$$

where we defined the PM 'field': $\tilde{E}_{pm} \equiv \tilde{F}_{pm}/(-e)$.

In the framework of a single-mode interaction model, we keep in the summation of eqn [30] only one mode q (usually the fundamental mode, and in free space – a Gaussian mode). The transverse current density components in eqn [31] $\tilde{J}_\perp = \frac{1}{2}\tilde{\rho}\,\tilde{v}_w^*$ are found using eqns [22], [33], and [36]. Finally, substituting $C_q(z) = \tilde{C}_q\,e^{i\delta kz}$ (where $\delta k \equiv k_z - k_{qz}$ and $k_z \cong k_{qz}$ is the wavenumber of the radiation wave modified by the interaction with the electrons) results in the general FEL dispersion relation:

$$(k_z - k_{zq})[1 + \chi_p(k_z + k_w, \omega)/\varepsilon] = \kappa\chi_p(k_z + k_w, \omega)/\varepsilon_0 \qquad [37]$$

Equation [37] is a general expression, valid for a wide variety of FELs, including Cerenkov–Smith–Purcell and TWT. They differ only in the expression for κ. For the conventional (magnetic wiggler) FEL:

$$\kappa = \frac{1}{8}\frac{A_e}{A_{em}}\frac{a_w^2}{\gamma^2\beta_z^2}\frac{\omega}{c}A_{JJ}^2 \qquad [38]$$

where A_e is the cross-section area of the electron beam, and $A_{em} \equiv \mathcal{P}_q/[\frac{1}{2}\sqrt{\varepsilon_0/\mu_0}|\varepsilon_{q\perp}(0,0)|^2]$ is the effective area of the interacting radiation-mode q, and it is assumed that the electron beam, passing on axis $(x_e, y_e) = (0,0)$, is narrow relative to the transverse mode variation $A_e/A_{em} \ll 1$. The 'Bessel-functions coefficient' A_{JJ} is defined for a linear wiggler only, and is given by:

$$A_{JJ} = J_0\left[\frac{a_w^2}{2(a_w^2+2)}\right] - J_1\left[\frac{a_w^2}{2(a_w^2+2)}\right] \qquad [39]$$

In a helical wiggler, $A_{JJ} \equiv 1$. Usually $a_w \ll 1$, and therefore $A_{JJ} \cong 1$.

The Pierce Dispersion Equation

The longitudinal plasma response susceptibility function $\chi_p(k_z, \omega)$ has been calculated, in any plasma formulation, including fluid model, kinetic model, or

even quantum-mechanical theory. If the electron beam axial velocity spread is small enough (cold beam), then the fluid plasma equations can be used. The small signal longitudinal force equation derived from eqn [25], together with eqn [33] and the small signal current modulation expression:

$$\tilde{J}_z \cong \rho_0 \tilde{v}_z + v_z \tilde{\rho} \qquad [40]$$

result in:

$$\chi_p(k_z, \omega) = -\frac{\omega_p'^2}{(\omega - k_z v_z)^2} \varepsilon_0 \qquad [41]$$

where $\omega_p' = (e^2 n_0/\gamma\gamma_z^2 \varepsilon m)^{1/2}$ is the longitudinal plasma frequency, n_0 is the beam electrons density ($\rho_0 = -en_0$), v_z is the average axial velocity of the beam.

In this 'cold-beam' limit, the FEL dispersion eqn [37] reduces into the well-known 'cubic dispersion equation' derived first by John Pierce in the late 1940s for the TWT:

$$\delta k(\delta k - \theta - \theta_{pr})(\delta k - \theta + \theta_{pr}) = -Q \qquad [42]$$

where $\delta k = k_z - k_{zq}$, θ is the detuning parameter (off the synchronism condition of eqn [24]):

$$\theta \equiv \frac{\omega}{v_z} - k_{zq} - k_w \qquad [43]$$

$$\theta_p = \frac{\omega_p'}{v_z} \qquad [44]$$

$$Q = \kappa \theta_p^2 \qquad [45]$$

Here $\theta_{pr} = r_p \theta_p$, where $r_p < 1$ is the plasma reduction factor. It results from the reduction of the longitudinal space-charge field $\tilde{E}_{sp}$ in a beam of finite radius r_b due to the fringe field effect ($r_p \to 1$ when the beam is wide relative to the longitudinal modulation wavelength: $r_b \gg \lambda_{pm} = 2\pi/(k_{zq} + k_w)$).

The cubic equation has, of course, three solutions δk_i ($i = 1, 2, 3$), and the general solution for the radiation field amplitude and power is thus:

$$C_q(z) = \sum_{j=1}^{3} A_j e^{i\delta k_j z} \qquad [46]$$

$$P(z) = |C_q(z)|^2 \mathcal{P}_q \qquad [47]$$

The coefficients A_i can be determined from three initial conditions of the radiation and e-beam parameters $C_q(0)$, $\tilde{v}(0)$, $\tilde{i}(0)$, and can be given as a linear combination of them (here $\tilde{i} = A_e \tilde{J}_z$ is the longitudinal modulation current):

$$A_j = B_j^E(\omega) C_q^\omega(0) + B_j^v(\omega) \tilde{v}^\omega(0) + B_j^i(\omega) \tilde{i}^\omega(0) \qquad [48]$$

Alternatively stated, the exit amplitude of the electromagnetic mode can in general be expressed in terms of the initial conditions:

$$C_q(L) = H^E(\omega) C_q(\omega, 0) + H^v(\omega) \tilde{v}(\omega, 0) + H^i(\omega) \tilde{i}(\omega, 0) \qquad [49]$$

where

$$H^{(E,v,i)}(\omega) = \sum_{j=1}^{3} B_j^{(E,v,i)}(\omega) e^{i\delta k_j L} \qquad [50]$$

In the conventional FEL, electrons are injected in randomly, and there is no velocity prebunching ($\tilde{v}(\omega, 0) = 0$) or current prebunching ($\tilde{i}(\omega, 0) = 0$) (or equivalently $\tilde{n}(\omega, 0) = 0$). Consequently, $C_q(z)$ is proportional to $C_q(0)$ and one can define and calculate the FEL small-signal single-path gain parameter:

$$G(\omega) \equiv \frac{P(L)}{P(0)} = \frac{|C_q(\omega, L)|^2}{|C_q(\omega, 0)|^2} = |H^E(\omega)|^2 \qquad [51]$$

The FEL Gain Regimes

At different physically meaningful operating regimes, some parameters in eqn [42] can be neglected relative to others, and simple analytic expressions can be found for δk_i, A_i, and consequently $G(\omega)$. It is convenient to normalize the FEL parameters to the wiggler length: $\bar{\theta} = \theta L$, $\bar{\theta}_{pr} = \theta_{pr} L$, $\bar{Q} = QL^3$. An additional figure of merit parameter is the 'thermal' spread parameter:

$$\bar{\theta}_{th} = \frac{v_{zth}}{v_z} \frac{\omega}{v_z} L \qquad [52]$$

where v_{zth} is the axial velocity spread of the e-beam (in a Gaussian velocity distribution model: $f(v_z) = \exp[(v_z - v_{z0})/v_{zth}]/\sqrt{\pi} v_{zth}$). The axial velocity spread can result out of beam energy spread or angular spread (finite 'emittance'). It should be small enough, so that the general dispersion relation of eqn [37] reduces to eqn [42] (the practical 'cold beam' regime).

Assuming now a conventional FEL ($\tilde{v}_z(0) = 0$, $\tilde{i}(0) = 0$), the single path gain in eqn [51] can be calculated. We present next this gain expression in the different regimes. The maximum values of the gain expression in the different regimes are listed in Table 1.

Low gain

This is the regime where the differential gain in a single path satisfies $G - 1 = [P(L) - P(0)]/P(0) \ll 1$. It is not useful for FEL amplifiers but most FEL oscillators operate in this regime.

Table 1 The gain regimes maximum gain expressions

	Gain regime	*Parameters domain*	*Max. gain expression*
I	Tenuous beam low-gain	$\bar{Q},\ \bar{\theta}_{pr},\ \bar{\theta}_{th} < \pi$	$\frac{P(L)}{P(0)} = 1 + 0.27\bar{Q}$
II	Collective low-gain	$\bar{\theta}_{pr} > \frac{\bar{Q}}{2},\ \bar{\theta}_{th},\ \pi$	$\frac{P(L)}{P(0)} = 1 + \bar{Q}/2\bar{\theta}_{pr}$
III	Collective high-gain	$\bar{Q}/2 > \bar{\theta}_{pr} > \bar{Q}^{1/3},\ \bar{\theta}_{th},\ \bar{Q} > \pi$	$\frac{P(L)}{P(0)} = \frac{1}{4}\exp(\sqrt{2\bar{Q}/\bar{\theta}_{pr}})$
IV	Strong coupling high-gain	$\bar{Q}^{1/3} > \bar{\theta}_{pr},\ \bar{\theta}_{th},\ \bar{Q} > \pi$	$\frac{P(L)}{P(0)} = \frac{1}{9}\exp(\sqrt{3}\bar{Q}^{1/3})$
V	Warm beam	$\bar{\theta}_{th} > \bar{\theta}_{pr},\ \bar{Q}^{1/3},\ \pi$	$\frac{P(L)}{P(0)} = \exp(3\bar{Q}/\bar{\theta}_{th}^2)$

The three solutions of eqn [42] – namely the terms of eqn [46] – are reminiscent of the three eigenwaves of the uncoupled system ($\kappa = Q = 0$) : the radiation mode and the two plasma (space-charge) waves of the e-beam (the slow and fast waves, corresponding respectively to the forward and backward propagating plasma-waves in the beam rest reference-frame). In the low-gain regime, all three terms in eqn [46] are significant. Calculating them to first order in κ, results in analytical gain expressions in the collective ($\bar{\theta}_{pr} \gg \pi$) and tenuous-beam ($\bar{\theta}_{pr} \ll \pi$) regimes (note that $\bar{\theta}_{pr}/2\pi = f'_{pr}L/v_z$ is the number of plasma oscillations within the wiggler transit time L/v_z).

In most practical situations the beam current density is small enough, and its energy high enough, to limit operation to the tenuous-beam regime. The gain curve function is then:

$$G(\omega) - 1 = \bar{Q}F(\bar{\theta}(\omega)) = \bar{Q}\frac{d}{d\bar{\theta}}\mathrm{sinc}^2(\bar{\theta}/2) \qquad [53]$$

$$\bar{\theta}(\omega) \equiv \theta(\omega)L = 2\pi\frac{\omega - \omega_0}{\Delta\omega_L} \qquad [54]$$

where $\mathrm{sinc}(u) \equiv (\sin u)/u$, and in free space (no waveguide) propagation ($k_{zq} = \omega/c$), the FWHM frequency bandwidth of the $\mathrm{sinc}^2(\bar{\theta}/2)$ function is:

$$\frac{\Delta\omega_L}{\omega_0} = \frac{1}{N_w} \qquad [55]$$

The small signal gain curve is shown in Figure 8. There is no gain at synchronism – $\omega = \omega_0$. Maximum gain – $G - 1 = 0.27\bar{Q}$, is attained at a frequency slightly smaller than ω_0, corresponding to $\bar{\theta} = -2.6$. The small gain curve bandwidth is $\Delta\omega_{SG} \cong \Delta\omega_L/2$,

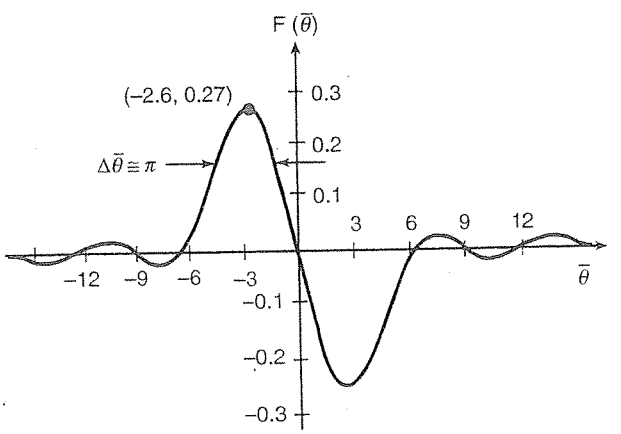

Figure 8 The low-gain cold-beam small-signal gain curve of FEL as a function of the detuning parameter $\bar{\theta}(\omega)$.

namely:

$$\frac{\Delta\omega_{SG}}{\omega_0} = \frac{1}{2N_w} \qquad [56]$$

High gain

This is the regime where the FEL gain in a single path satisfies $G = P(L)/P(0) \gg 1$. It is useful, of course, when the FEL is used as an amplifier.

Since the coefficients of the cubic eqn [42] are all real, the solutions δk_i ($i = 1, 2, 3$) must be either all real, or composed of one real solution δk_3 and two complex solutions, which are complex conjugate of each other: $\delta k_1 = \delta k_2^*$. In the first case, all terms in eqn [46] are purely oscillatory, there is no exponential growth, and the FEL operates in the low gain regime. In the second case, assuming $\mathrm{Im}(\delta k_1) < 0$, $\mathrm{Im}(\delta k_2) > 0$, the first term grows exponentially, and if L is long enough it will dominate over the other decaying ($j = 2$) and oscillatory ($j = 3$) terms, and

result in an exponential gain expression:

$$G(\omega) = \left(\frac{A_1}{A_1 + A_2 + A_3}\right)^2 e^{2(\mathrm{Im}\,\delta k_1)L} \qquad [57]$$

If we focus on the tenuous-beam strong coupling (high-gain) regime $\theta_{pr} \ll |\delta k|$, then the cubic eqn [42] gets the simple form:

$$\delta k(\delta k - \theta)^2 = -\Gamma^3 \qquad [58]$$

where

$$\Gamma = Q^{1/3} = \left(\frac{\pi}{2}\frac{a_w^2}{\gamma^3\gamma_z^2\beta_z^5}\frac{\omega/c}{A_{em}}\frac{I_b}{I_A}A_{JJ}^2\right)^{1/3} \qquad [59]$$

and $I_A = 4\pi\varepsilon_0 m_e c^3/e \cong 17$ kA is the Alfven current. The solution of eqn [58] near synchronism ($\theta \cong 0$) is:

$$\delta k_1 = \frac{1 - \sqrt{3}i}{2}\Gamma, \qquad \delta k_2 = \frac{1 + \sqrt{3}i}{2}\Gamma, \qquad \delta k_3 = -\Gamma \qquad [60]$$

resulting in:

$$H^E(\omega) = \frac{C_q(z)}{C_q(0)} = \frac{1}{3}\left[e^{\frac{\sqrt{3}+i}{2}\Gamma z} + e^{\frac{-\sqrt{3}+i}{2}\Gamma z} + e^{-i\Gamma z}\right] \qquad [61]$$

and for $\Gamma L \gg 1$:

$$G \cong \frac{1}{9}e^{\sqrt{3}\Gamma L} \qquad [62]$$

The FEL gain is then exponential and can be very high. The gain exponential coefficient is characterized then by its third-order root scaling with the current, $\alpha I_b^{1/3}$. The high-gain frequency detuning curve (found by solving eqn [58] to second order in θ) is:

$$G \cong \frac{1}{9}e^{\sqrt{3}\Gamma L}\exp(-\vec{\theta}^2/\Gamma L 3^{3/2}) \equiv \frac{1}{9}e^{\sqrt{3}\Gamma L}\exp\left[-\frac{(\omega - \omega_0)^2}{\Delta\omega_{HG}^2}\right] \qquad [63]$$

where $\Delta\omega_{HG}$ is the 1/e half-width of the gain curve:

$$\frac{\Delta\omega_{HG}}{\omega_0} = \frac{3^{3/4}}{2\pi}\frac{\lambda_w}{(L/\Gamma)^{1/2}} \qquad [64]$$

Super-Radiance, Spontaneous-Emission and Self Amplified Spontaneous Emission (SASE)

Intense coherent radiation power can be generated in a wiggler or any other radiation scheme without any input radiation signal ($C_q(\omega, 0) = 0$) if the electron beam velocity or current (density) are prebunched. Namely, the injected e-beam has a frequency component $\tilde{v}(\omega)$ or $\tilde{i}(\omega)$ in the frequency range where the radiation device emits. In the case of pure density bunching ($\tilde{v}(\omega) = 0$), the coherent power emitted is found from eqns [46, 47, 49]:

$$(P_q)_{SR} = P_q|H^i(\omega)|^2|\tilde{i}(\omega, 0)|^2 \qquad [65]$$

A 'prebunched-beam FEL' emits coherent radiation based on the process of Super-radiant Emission (in the sense of Dike). Because all electrons emit in phase radiation wavepackets into the radiation mode, the resultant field amplitude is proportional in this case to I_b and the radiation power – to I_b^2. By contrast, spontaneous emission from a random electron beam (no bunching) is the result of incoherent superposition of the wavepackets emitted by the electrons and its power is expected to be proportional to the current I_b.

When the current to radiation field transfer function $H^i(\omega)$ is known, eqn [65] can be used to calculate the superradiant power, and in the high-gain regime also the amplified-superradiant power. The latter is the amplification of the superradiant radiation in the downstream sections of a long wiggler. Such unsaturated gain is possible only when the beam is partly bunched $|\tilde{i}(\omega)| \sim I_b$ (because the FEL gain process requires enhanced bunching).

The expressions for the current to field transfer function, in the superradiant gain and the high-gain amplified superradiance limits respectively, are:

$$|H^i(\omega)| = \frac{(P_{pb}/P_q)^{1/2}}{I_b}\mathrm{sinc}(\theta L/2) \qquad [66]$$

$$|H^i(\omega)| = \frac{(P_{pb}/P_q)^{1/2}}{3\Gamma L I_b}e^{(\sqrt{3}/2)\Gamma L}\,e^{-(\omega-\omega_0)^2/2(\Delta\omega)_{HG}^2} \qquad [67]$$

where

$$P_{pb} = \frac{I_b^2\sqrt{\mu_0/\varepsilon_0}}{32}\left(\frac{a_w}{\gamma\beta_z}\right)^2\frac{L^2}{A_{em}} \qquad [68]$$

From these expressions one can calculate the power and spectral power of both coherent (superradiant) and partially coherent (spontaneous emission) radiation of FEL in the negligible gain and high gain regimes. The corresponding super-radiant power is in the negligible superradiance gain limit:

$$P_{SR} = P_{pb}\left|\frac{\tilde{i}(\omega)}{I_b}\right|^2\mathrm{sinc}^2(\theta L/2) \qquad [69]$$

(proportional, as expected, to the modulation current squared) and in the high-gain amplified superradiance limit (assuming initial partial bunching $|i(\omega)/I\mathrm{b}| \ll 1$):

$$P_{SR} = P_{pb}\left|\frac{\tilde{i}(\omega)}{I_b}\right|^2 \frac{1}{9(\Gamma L)^2} e^{\sqrt{3}\Gamma L}\, e^{-(\omega-\omega_0)^2/(\Delta\omega)^2_{HG}} \quad [70]$$

The discussion is now extended to incoherent (or partially coherent) spontaneous emission. Due to its particulate nature, every electron beam has random frequency components in the entire spectrum (shot noise). Consequently, incoherent radiation power is always emitted from an electron-beam passing through a wiggler, and its spectral-power can be calculated through the relation:

$$\frac{dP_q}{d\omega} = \frac{2}{\pi}\mathcal{P}_q|H^i(\omega)|^2\frac{\langle|\tilde{i}(\omega)|^2\rangle}{T} \quad [71]$$

Here $\tilde{i}(\omega)$ is the Fourier transform of the current of randomly injected electrons $i(t) = -e\sum_{j=1}^{N_T}\delta(t - t_{oj})$, where N_T is the average number of electrons in a time period T, namely, the average (DC) current is $I_b = -eN_T/T$. For a randomly distributed beam, the shot noise current is simply $\langle|i(\omega)|^2\rangle/T = eI_b$, and therefore the spontaneous emission power of the FEL, which is nothing but the 'synchrotron-undulator radiation', is given by (see eqn [66]):

$$\frac{dP_q}{d\omega} = \frac{1}{16\pi}eI_bZ_q\frac{L^2}{A_{em}}\left(\frac{a_w}{\gamma\beta_z}\right)^2 \mathrm{sinc}^2(\theta L/2) \quad [72]$$

If the wiggler is long enough, the spontaneous emission emitted in the first part of the wiggler can be amplified by the rest of it (SASE). In the high-gain limit (see eqn [67]), the amplified spontaneous emission power within the gain bandwidth of eqn [64] is given by:

$$P_q = \frac{2}{\pi}\mathcal{P}_q eI_b\int_0^\infty |H^i(\omega)|^2 d\omega = \frac{1}{9}P_{sh}\, e^{\sqrt{3}\Gamma L} \quad [73]$$

where P_{sh} is an 'effective shot-noise input power':

$$P_{sh} = \frac{2}{\sqrt{\pi}}\frac{eP_{pb}}{I_0(\Gamma L)^2}(\Delta\omega)_{HG} \quad [74]$$

Saturation Regime

The FEL interaction of an electron with an harmonic electromagnetic (EM) wave is essentially described by the longitudinal component of the force in eqn [25], driven by the pondermotive force of eqns [27] and [28]:

$$\frac{d}{dt}(\gamma_i m v_{zi}) = \left|\tilde{F}_{pm}\right|\cos[\omega t - (k_z + k_w)z_i] \quad [75]$$

$$dz_i/dt = v_{zi} \quad [76]$$

As long as the interaction is weak enough (small signal regime), the change in the electron velocity is negligible – $v_{zi} \cong v_{z0}$, and the phase of the force-wave, experienced by the electron, is linear in time $\Psi_i(t) = [\omega - (k_z + k_w)v_{z0}](t - t_{0i}) + \omega t_{0i}$. Near synchronism condition $\theta \cong 0$ (eqn [24]), eqn [75] results in bunching of the beam, because different acceleration/deceleration forces are applied on each electron, depending on their initial phase $\Psi_i(0) = \omega t_{0i}(-\pi < \Psi_i(0) < \pi)$ within each optical period $2\pi/\omega$ (see Figure 7). Taylor expansion of v_{zi} around v_{z0} in eqns [75] and [76], and use of conservation of energy between the e-beam and the radiation field, would lead again to the small signal gain expression eqn [53] in the low gain regime.

When the interaction is strong enough (the non-linear or saturation regime), the electron velocities change enough to invalidate the assumption of linear time dependence of Ψ_i and the nonlinear set of eqns [75] and [76] needs to be solved exactly.

It is convenient to invert the dependence on time $z_i(t) = \int_{t_{0i}}^{t} v_{zi}(t')dt'$, and turn the coordinate z to the independent variable $t_i(z) = \int_0^z dz'/v_{zi}(z') + t_{0i}$. This, and direct differentiation of $\gamma_i(v_{zi})$, reduces eqns [75] and [76] into the well-known pendulum equation:

$$\frac{d\theta_i}{dz} = -K_s^2 \sin\Psi_i \quad [77]$$

$$\frac{d\Psi_i}{dz} = \theta_i \quad [78]$$

where

$$\Psi_i = \int_0^z (\omega/v_{zi}(z') - k_z - k_w)\, dz' \quad [79]$$

$$\theta_i = \frac{\omega}{v_{zi}} - k_z - k_w \quad [80]$$

are respectively the pondermotive potential phase and the detuning value of electron i at position z.

$$K_s = \frac{k\sqrt{a_w a_s A_{JJ}/2}}{\gamma_0\gamma_{z0}\beta_{z0}^2} \quad [81]$$

is the synchrotron oscillation wavenumber, where a_w is given in eqn [9], $a_s = e|\tilde{E}_s|/\omega mc$, and $\gamma_0 = \gamma(0)$, $\gamma_{z0} = \gamma_z(0)$, and $\beta_{z0} = \beta_z(0)$ are the initial parameters of the assumed cold beam.

The pendulum eqns [77] and [78] can be integrated once, resulting in:

$$\tfrac{1}{2}\theta_i^2(z) - K_s^2\cos\Psi_i(z) = C_i \quad [82]$$

and the integration constant is determined for each electron by its detuning and phase relative to the

pondermotive wave at the entrance point ($z = 0$): $C_i = \frac{1}{2}\theta_i^2(0) - K_s^2\cos\Psi_i(0)$.

The $\theta(z)$, $\Psi(z)$ phase-space trajectories of eqn [82] are shown in **Figure 9** for various values of C_i (corresponding to the initial conditions $\theta_i(0)$, $\Psi_i(0)$). The trajectories corresponding to $|C_i| > K_s^2$ are open; namely electrons on these trajectories, while oscillating, can slip-off out of the pondermotive–potential wave period to adjacent periods, ahead or backward, depending on the value of their detuning parameter $\bar{\theta}$. The trajectories corresponding to $|C_i| < K_s^2$ are closed, namely the electrons occupying these trajectories are 'trapped', and their phase displacement is bound to a range $|\Psi_i(z) - n\pi| < \Psi_{im} \equiv \arccos(|C_i|/K_s^2) < \pi$ within one pondermotive-wave period. The trajectory $C_i = K_s^2$ defines the 'separatrix':

$$\theta_i(z) = \pm 2K_s\cos(\Psi_i/2) \qquad [83]$$

which is sometimes referred to as the 'trap' or 'bucket'. Every electron within the separatrix stays trapped, and the ones out of it are free (untrapped). The height of the separatrix (maximum detuning swing) is $\Delta\theta_{trap} = 4K_s$. The oscillation frequency of the trapped electrons can be estimated for deeply trapped electrons ($\Psi_m \ll 2\pi$). In this case the physical pendulum eqns [77] and [78] reduce to the mathematical pendulum equation with an oscillation frequency K_s, in the z coordinate. This longitudinal oscillation, called 'synchrotron oscillation', takes place as a function of time at the 'synchrotron frequency' $\Omega_s = K_s v_z$.

Differentiation of $\theta_i(v_{zi})$ and $v_{zi}(\gamma_i)$ permits to describe the phase-space dynamics in terms of the more physical parameters $\delta v_{zi} = v_{zi} - v_{ph}$ and $\delta\gamma_i = \gamma_i - \gamma_{ph}$, where:

$$v_{ph} = \frac{\omega}{k_z + k_w} \qquad [84]$$

is the phase velocity of the pondermotive wave and $\gamma_{ph} \equiv (1 - \beta_{ph}^2)^{-1/2}$:

$$-\theta_i = \frac{\omega}{c^2\beta_{z0}^2}\delta v_{zi} = \frac{k}{\beta_{z0}^3\gamma_{z0}^2\gamma_0}\delta\gamma_i \qquad [85]$$

Figure 10 displays a typical dynamics of electron beam phase-space (γ, Ψ) evolution for the case of a cold beam of energy $\gamma(0)$ entering the interaction region at $z = 0$ with uniform phase distribution (random arrival times t_{0i}). The FEL is assumed to operate in the low-gain regime (typical situation in an FEL oscillator), and, therefore, the trap height (corresponding to $\Delta\theta_{trap} = 4K_s$):

$$\Delta\gamma_{trap} = 8\beta_z^2\gamma_z^2\gamma K_s/k \qquad [86]$$

remains constant along the interaction length. **Figure 10a** displays the e-beam phase-space evolution in the small signal regime. The uniform phase distribution evolves along the wiggler into a bunched distribution (compare to **Figure 7c**), and its average kinetic energy goes down $(\Delta E_k) = [\langle\gamma_i(L)\rangle - \gamma(0)]mc^2 < 0$, contributing this energy to the field of the interacting radiation mode, $\Delta P_q = (\Delta E_k)I_0/e$. In this case (corresponding in an FEL oscillator to the early stages of oscillation build-up), the electrons remain free (untrapped) along the entire length L.

Figure 10b displays the e-beam phase-space evolution in the large signal (saturation) regime (in the case of an oscillator – at the steady-state saturation stage). Part of the electrons are found inside the trap, immediately upon entering the interaction region ($z = 0$), and they lose energy of less than (but near) $mc^2\Delta\gamma_{trap}$ as they pass through the interaction region ($z = L$). A portion of the electrons remain outside the traps upon entrance. They follow open trajectories and lose less energy or may even become accelerated due to their interaction with the wave.

It can be appreciated from this discussion that a good design strategy in attempting to extract maximum power from the electron beam in the FEL interaction, is to set the parameters determining the synchrotron oscillation frequency K_s in eqn [81] so that only half a synchrotron oscillation period will be performed along the interaction length:

$$K_s L = \pi \qquad [87]$$

This is controlled in an amplifier by keeping the input radiation power $P_q(0)$ (and consequently a_s) small enough, so that K_s will not exceed the value set

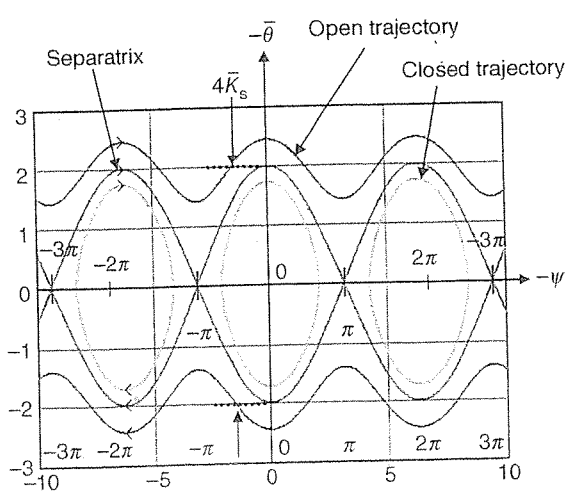

Figure 9 The $(\theta-\Psi)$ phase-space trajectories of the pendulum equation.

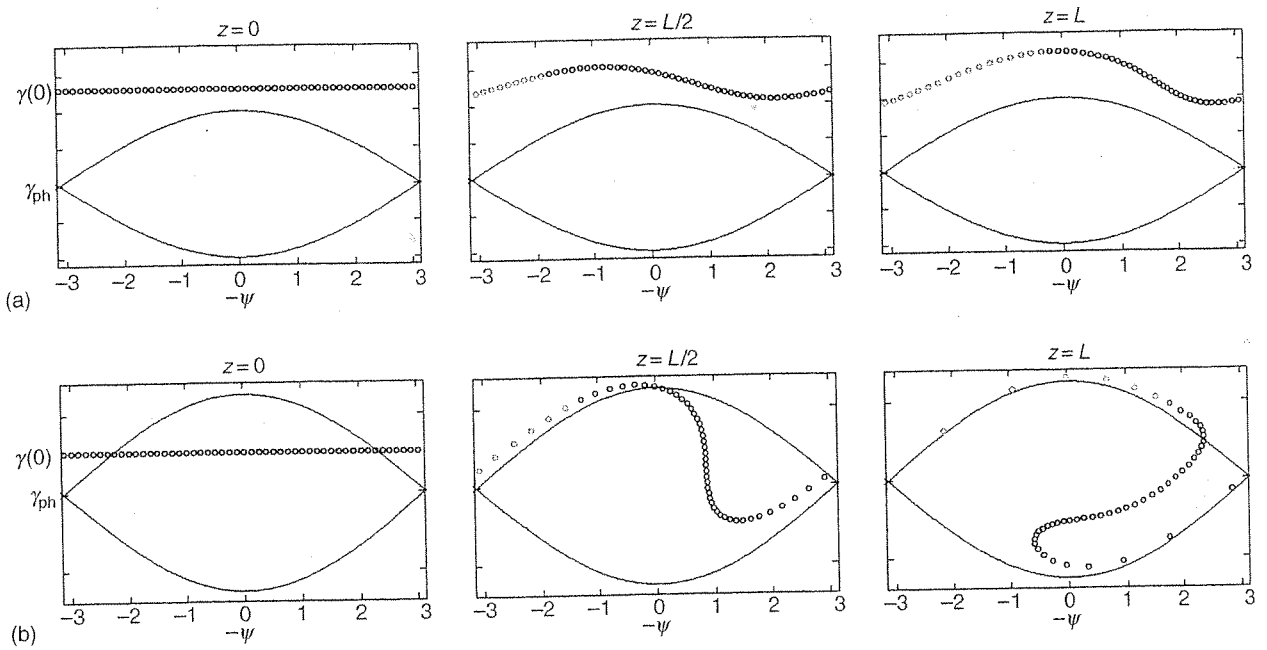

Figure 10 'Snapshots' of the (γ–Ψ) phase-space distribution of an initially uniformly distributed cold beam relative to the PM-wave trap at three points along the wiggler (a) Moderate bunching in the small-signal low gain regime. (b) Dynamics of electron beam trapping and synchrotron oscillation at steady state saturation stage of a FEL oscillator ($K_s L = \pi$).

by eqn [87]. In an oscillator, this is controlled by increasing the output mirror transmission sufficiently, so that the single path incremental small signal gain G-1 will not be much larger than the round trip loss, and the FEL will not get into deep saturation. When the FEL is over-saturated ($K_s L > \pi$), the trapped electrons begin to gain energy as they continue to rotate in their phase-space trajectories beyond the lowest energy point of the trap, and the radiative energy extraction efficiency drops down.

A practical estimate for the FEL saturation power emission and radiation extraction efficiency can be derived from the following consideration: the electron beam departs from most of its energy during the interaction with the wave, if a significant fraction of the electrons are within the trap and have positive velocity δv_{zi} relative to the wave velocity v_{ph} at $z = 0$, and if at the end of the interaction length ($z = L$), they complete half a pendulum swing and reverse their velocity relative to the wave $\delta v_{zi}(L) \cong -\delta v_{zi}(0)$. Correspondingly, in the energy phase-space diagram (**Figure 10b**) the electrons perform half a synchrotron oscillation swing and $\delta\gamma_i(L) = \gamma_i(L) - \gamma_{ph} = -\delta\gamma_i(0)$. In order to include in this discussion also the FEL amplifier (in the high gain regime), we note that in this case the phase velocity of the wave v_{ph} in eqn [84], and correspondingly γ_{ph}, are modified by the interaction contribution to the radiation wavenumber – $k_z = k_{z0} + \mathrm{Re}(\delta k)$, and also the electron detuning parameter (relative to the pondermotive wave) θ_i in eqn [80] differs from the beam detuning parameter θ in eqn [43]: $\theta_i = \theta - \mathrm{Re}(\delta k)$. Based on these considerations and eqn [85], the maximum energy extraction from the beam in the saturation process is:

$$\Delta\gamma = 2\delta\gamma_i(0) = 2\beta_{z0}^3\gamma_{z0}^2\gamma_0\frac{\mathrm{Re}\,\delta k - \theta}{k} \qquad [88]$$

where θ is the initial detuning parameter in eqn [43].

In an FEL oscillator, operating in general in the low-gain regime, $|\mathrm{Re}\,\delta k| \ll |\theta|$, oscillation will start usually at the resonator mode frequency, corresponding to the detuning parameter $\theta(\omega) = -2.6/L$, for which the small signal gain is maximal (see **Figure 8**). Then the maximum radiation extraction efficiency can be estimated directly from eqn [88]. It is, in the highly relativistic limit ($\beta_{z0} \cong 1$):

$$\eta_{ext} = \frac{\Delta\gamma}{\gamma_0} \cong \frac{1}{2N_w} \qquad [89]$$

In an FEL amplifier, in the high-gain regime $\mathrm{Re}\,\delta k = \Gamma/2 \gg |\theta|$, and consequently in the same limit:

$$\eta_{ext} \cong \frac{\Gamma\lambda_w}{4\pi} \qquad [90]$$

It may be interpreted that the effective wiggler length for saturation is $L_{eff} = 2\pi/\Gamma$.

Equation [90], derived here for a coherent wave, is considered valid also for estimating the saturation

efficiency also in SASE-FEL. In this context, it is also called 'the efficiency parameter' $-\rho$.

FEL Radiation Schemes and Technologies

Contrary to conventional atomic and molecular lasers, the FEL operating frequency is not determined by natural discrete quantum energy levels of the lasing matter, but by the synchronism condition of eqn [24] that can be predetermined by the choice of wiggler period, $\lambda_w = 2\pi/k_w$, the resonator dispersion characteristics $k_{zq}(\omega)$, and the beam axial velocity v_z.

Because the FEL design parameters can be chosen at will, its operating frequency can fit any requirement, and furthermore, it can be tuned over a wide range (primarily by varying v_z). This feature of FEL led to FEL development efforts in regimes where it is hard to attain high-power tunable conventional lasers or vacuum-tube radiation sources – namely in the sub-mm (far infrared or THz) regimes, and in the VUV down to soft X-ray wavelengths.

In practice, in an attempt to develop short wavelength FELs, the choice of wiggler period λ_w is limited by an inevitable transverse decay of the magnetic field away from the wiggler magnets surface (a decay range of $\approx k_w^{-1}$) dictated by the Maxwell equations. To avoid interception of electron beam current on the walls or on the wiggler surfaces, typical wiggler periods are made longer than $\lambda_w > 1$ cm. FELs (or FEMs – free electron masers) operating in the long wavelengths regime (mm and sub-mm wavelengths) must be based on waveguide resonators to avoid excessive diffraction of the radiation beam along the interaction length (the wiggler). This determines the dispersion relation $k_{zq}(\omega) = (\omega^2 - \omega_{coq}^2)^{1/2}/c$ where ω_{coq} is the waveguide cutoff frequency of the radiation mode q. The use of this dispersion relation in eqn [24] results in an equation for the FEL synchronism frequency ω_0. Usually the fundamental mode in an overmoded waveguide is used (the waveguide is overmoded because it has to be wide enough to avoid interception of electron beam current). In this case ($\omega_0 \gg \omega_{co}$) and certainly in the case of an open resonator (common in FELs operating in the optical regime), $k_{zq} = \omega/c$, and the synchronism condition in eqn [24] simplified to the well-known FEL radiation wavelength expression in eqn [6]:

$$\lambda = (1 + \beta_z)\beta_z\gamma_z^2\lambda_w \cong 2\gamma_z^2\lambda_w \qquad [91]$$

where γ_z, a_w are defined in eqns [7]–[9].

To attain strong interaction, it is desirable to keep the wiggler parameter a_w large (eqn [38]), however, if $a_w > 1$, this will cause reduction in the operating wavelength according to eqns [7] and [91]. For this reason, and also in order to avoid harmonic frequencies emission (in case of a linear wiggler), $a_w < 1$ in common FEL design. Consequently, considering the practical limitations on λ_w, the operating wavelength eqn [91] is determined primarily by the beam relativistic Lorentz factor γ (eqn [8]).

The conclusion is that for a short wavelength FEL, one should use an electron beam accelerated to high kinetic energy E_k. Also, tuning of the FEL operating-wavelength can be done by changing the beam energy. Small-range frequency tuning can be done also by changing the spacing between the magnet poles of a linear wiggler. This varies the magnetic field experienced by the e-beam, and effects the radiation wavelength through change of a_w (see eqns [7] and [91]).

Figure 11 displays the operating wavelengths of FEL projects all over the world versus their e-beam energy. FELs were operated or planned to operate over a wide range of frequencies, from the microwave to X-ray – eight orders of magnitude. The data points fall on the theoretical FEL radiation curve eqns [7], [8], and [91].

FEL Accelerator Technologies

The kind of accelerator used is the most important factor in determining the FEL characteristics. Evidently, the higher the acceleration energy, the shorter is the FEL radiation wavelength. However, not only the acceleration beam energy determines the shortest operating wavelength of the FEL, but also the e-beam quality. If the accelerated beam has large energy spread, energy instability, or large emittance (the product of the beamwidth with its angular spread), then it may have large axial velocity spread v_{zth}. At high frequencies, this may push the detuning spread parameter $\bar{\theta}_{th}$ (eqn [52]) to the warm beam regime (see Table 1), in which the FEL gain is diminished, and FELs are usually not operated.

Other parameters of the accelerator determine different characteristics of the FEL. High current in the electron beam enables higher gain and higher power operation. The e-beam pulse shape (or CW) characteristics, affect, of course, the emitted radiation waveform, and may also affect the FEL gain and saturation characteristics. The following are the main accelerator technologies used for FEL construction. Their wavelength operating-regimes (eqn [91]) (determined primarily by their beam acceleration energies), are displayed in Figure 12.

Modulators and pulse-line accelerators

These are usually single pulse accelerators, based on high voltage power supplies and fast discharge stored

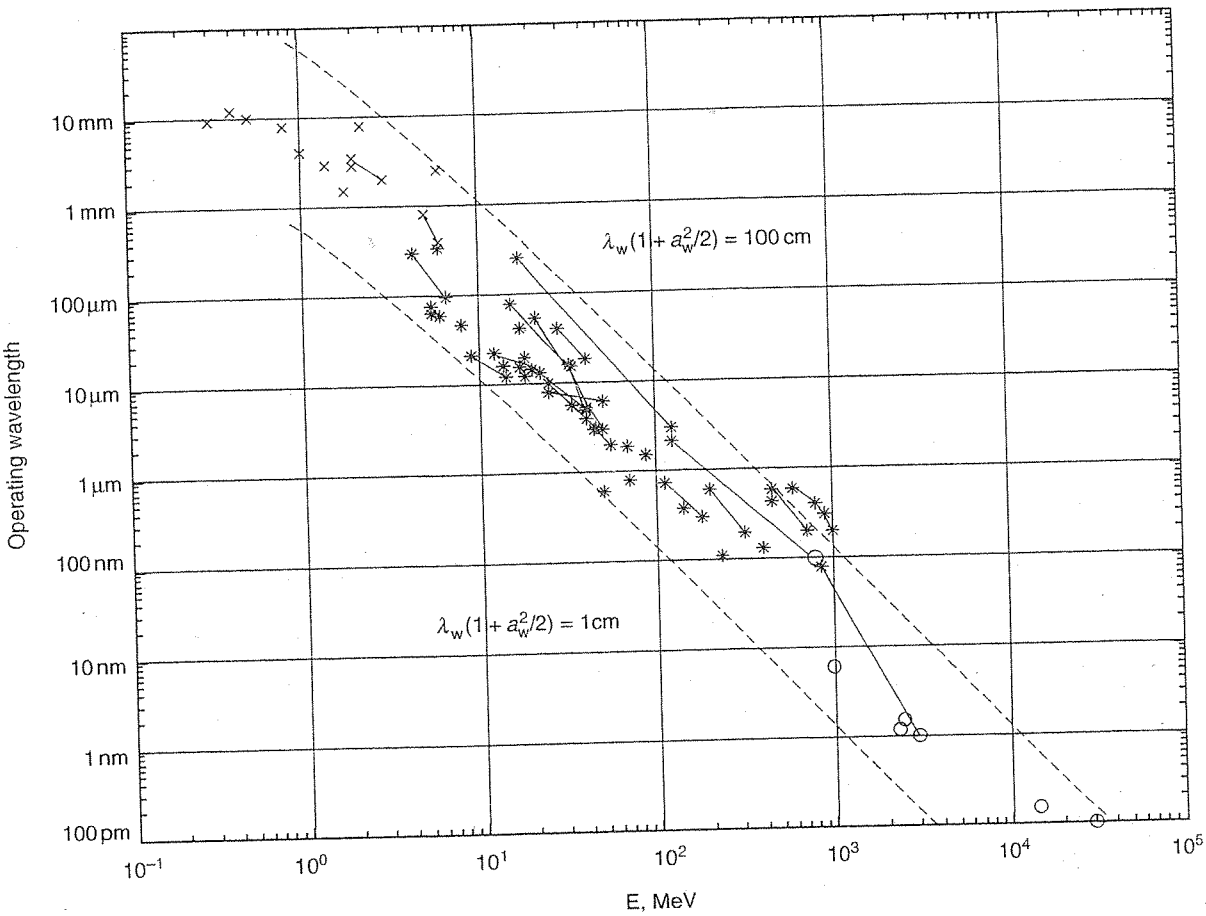

Figure 11 Operating wavelengths of FELs around the world vs. their accelerator beam energy. The data points correspond in ascending order of accelerator energy to the following experimental facilities: NRL (USA), IAP (Russia), KAERI (Korea), IAP (Russia), JINR/IAP (Russia), INP/IAP (Russia), TAU (Israel), FOM (Netherlands), KEK/JAERI (Japan/Korea), CESTA (France), ENEA (Italy), KAERI-FEL (Korea), LEENA (Japan), ENEA (Italy), FIR FEL (USA), mm Fel (USA), UCSB (USA), ILE/ILT (Japan), MIRFEL (USA), UCLA-Kurchatov (USA/Russia), FIREFLY (GB), JAERI-FEL (Japan), FELIX (Netherlands), RAFEL (USA), ISIR (Japan), UCLA-Kurchatov-LANL (USA/RU), ELSA (France), CLIO (France), SCAFEL (GB), FEL (Germany), BFEL (China), KHI-FEL (Japan), FELI4 (Japan), iFEL1 (Japan), HGHG (USA), FELI (USA), MARKIII (USA), ATF (USA), iFEL2 (Japan), VISA (USA), LEBRA (Japan), OK-4 (USA), UVFEL (USA), iFEL3 (Japan), TTF1 (Germany), NIJI-IV (Japan), APSFEL (USA), FELICITAI (Germany), FERMI (Italy), UVSOR (Japan), Super-ACO (France), TTF2 (Germany), ELETTRA (Italy), Soft X-ray (Germany), SPARX (Italy), LCLS (USA), TESLA (Germany). X, long wavelengths; *, short wavelengths; O, planned short wavelengths SASE-FELs. Data based in part on H. P. Freund, V. L. Granatstein, Nucl. Inst. and Methods In Phys. Res. A249, 33 (1999), W. Colson, Proc. of the 24th Int. FEL conference, Argone, III. (ed. K. J. Kim, S. V. Milton, E. Gluskin). The data points fall close to the theoretical FEL radiation condition expression (91) drawn for two practical limits of wiggler parameters.

electric energy systems (e.g., Marx Generator), which produce short pulse (tens of nSec) Intense Relativistic Beam (IRB) of energy in the range of hundreds of keV to few MeV and high instantaneous current (order of kAmp), using explosive cathode (plasma field emission) electron guns. FELs (FEMs), based on such accelerators, operated mostly in the microwave and mm-wave regimes. Because of their poor beam quality and single pulse characteristic, these FELs were, in most cases, operated only as Self Amplified Spontaneous Emission (SASE) sources, producing intense radiation beams of low coherence at instantaneous power levels in the range of 1–100 MW. Because of the high e-beam current and low energy, these FEMs operated mostly in the collective high-gain regime (see **Table 1**).

Some of the early pioneering work on FEMs was done in the 1970s and 1980s in the US (NRL, Columbia Univ., MIT), Russia (IAP), and France (Echole Politechnique), based on this kind of accelerators.

Induction linacs

These too are single pulse (or low repetition rate) accelerators, based on induction of electromotive potential over an acceleration gap by means of an electric-transformer circuit. They can be cascaded to high energy, and produce short pulse (tens to hundreds

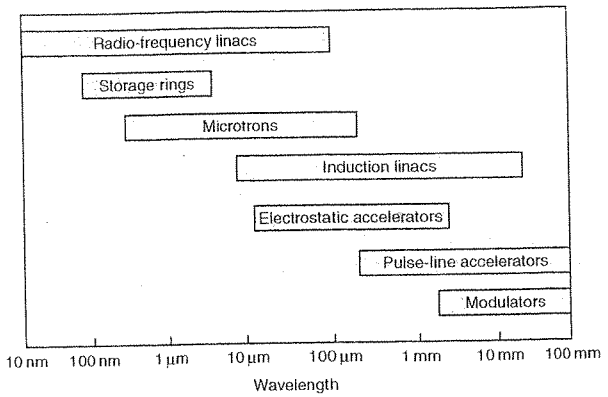

Figure 12 Approximate wavelength ranges accessible with FELs based on current accelerator and wiggler technologies.

of nSec), high current (up to 10 kA) electron beams, with relatively high energy (MeV to tens of MeV). The interest in FELs, based on this kind of accelerator technology, stemmed in the 1980s primarily from the SDI program, for the propose of development of a DEW FEL. The main development of this technology took place on a 50 MeV accelerator – ATA (for operating at 10 μm wavelength) and a 3.5 MeV accelerator – ETA (for operating at 8 mm wavelength). The latter experiment, operating in the high-gain regime, demonstrated record high power (1 GW) and energy extraction efficiency (35%).

Electrostatic accelerators

These accelerators are DC machines, in which an electron beam, generated by a thermionic electron-gun (typically 1–10 Amp) is accelerated electrostatically. The charging of the high voltage terminal can be done by mechanical charge transport (Van de Graaff) or electrodynamically (Crockford–Walton accelerator, Dynamitron). The first kind can be built at energies up to 25 MeV, and the charging current is less than mAmp. The second kind have terminal voltage less than 5 MeV, and the charging current can be hundreds of mAmps.

Because of their DC characteristics, FELs based on these kinds of accelerators can operate at arbitrary pulse shape structure and in principle – continuously (CW). However, because of the low charging current, the high electron beam current (1–10 Amp), required for FEL lasing must be transported without any interception along the entire way from the electron gun, through the acceleration tubes and the FEL wiggler, and then decelerated down to the voltage depressed beam-collector (multistage collector), closing the electric circuit back to the e-gun (current recirculation). The collector is situated at the e-gun potential, biased by moderate voltage high current power supplies, which deliver the current and power needed for circulating the e-beam and compensates for its kinetic energy loss in favor of the radiation field in the FEL cavity. This beam current recirculation is, therefore, also an 'Energy retrieval' scheme, and can make the overall energy transfer efficiency of the electrostatic-accelerator FEL very high.

In practice, high-beam transport efficiency in excess of 99.9% is needed for CW lasing, and has not been demonstrated yet. To avoid HV-terminal voltage drop during lasing, electrostatic-accelerator FELs are usually operated in a single pulse mode. Few FELs of this kind have been constructed. The first and main facility is the UCSB FEL shown in **Figure 13**. It operates in the wavelength range of 30 μm to 2.5 mm (with three switchable wigglers) in the framework of a dedicated radiation user facility. This FEL operates in the negatively charged terminal mode, in which the e-gun and collector are placed in the negatively charged HV-terminal inside the pressurized insulating gas tank, and the wigglers are situated externally at ground potential. An alternative operating mode of positively charged terminal internal cavity electrostatic-accelerator FEM was demonstrated in the Israeli Tandem–Accelerator FEM and the Dutch F.O.M. Fusion-FEM projects. This configuration enables operating with long pulse, high coherence, and very high average power. Linewidth of $\Delta\omega/\omega \cong 10^{-5}$ was demonstrated in the Israeli FEM and high power (730 kW over few microseconds) was demonstrated in the Dutch FEM, both at mm-wavelengths. The goal of the latter development project (which was not completed) was quasicontinuous operation at 1 MW average power for application in fusion plasma heating.

Radio-frequency (RF) accelerators

RF-accelerators are by far the most popular electron-beam sources for FELs. In RF accelerators, short electron beam bunches (bunch duration 1–10 pSec) are accelerated by the axial field of intense RF radiation (frequency about 1 GHz), which is applied in the acceleration cavities on the injected short e-beam bunches, entering with the accelerating-phase of the RF field. In microtrons, the electron bunches perform circular motion, and get incremental acceleration energy every time they re-enter the acceleration cavity. In RF-LINACs (linear accelerator), the electron bunches are accelerated in a sequence of RF cavities or a slow-wave structure, which keep an accelerating-phase synchronization of the traversing electron bunches with the RF field along a long linear acceleration length. The bunching of the electrons, prior to the acceleration step, is traditionally performed by bunching RF-cavities and a dispersive magnet (chicane) pulse compression system.

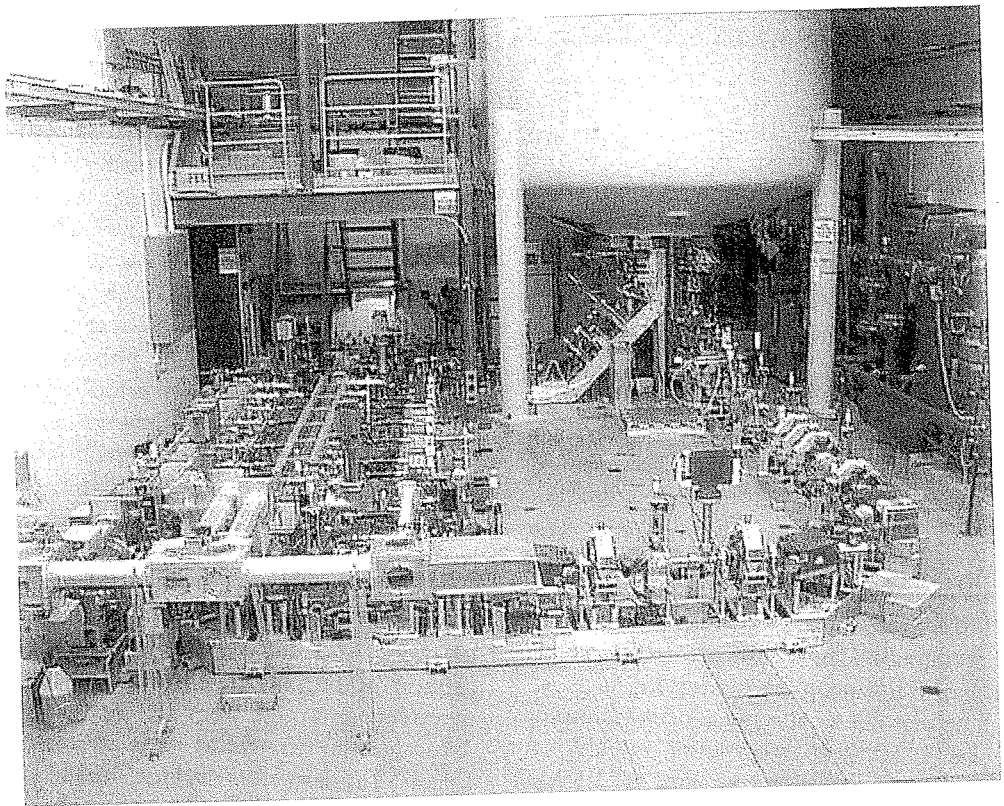

Figure 13 The UCSB 6MV Electrostatic – Accelerator FEL displaying the accelerator and a three-wigglers switchyard. Figure courtesy of the FEL Laboratory, University of California Santa, Barbara.

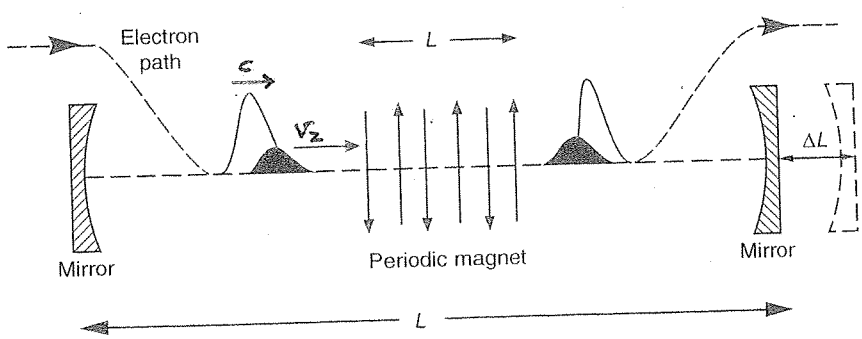

Figure 14 An FEL – Oscillator based on an RF accelerator electron bunches train. The resonator length L is tuned (ΔL) to attain best overlap between the electron bunch and the radiation wave pulse, which is slipping ahead through it. Reproduced from Colson WB (1982) Free-electron generators of coherent radiation. In: Jacobs SF *et al. Physics of Quantum Electronics*, vol. 8, p. 457. Reading, MA: Addison-Wesley.

Recent development of ultrashort-pulse intense UV sources, based on nonlinear optical multiplication of mode-locked solid state laser sources, makes it possible to attain excellent initial bunching (picoSecond and sub-picoSecond pulse durations with hundreds of ampere peak current) using photocathode electron-gun injectors (often integrated with a short accelerating RF cavity section.

Common normal-cavity RF-LINACS have energies of tens of MeV to GeV. Their electron beam current waveforms are determined by the characteristics of the klystrons that supply the acceleration RF power. Continous acceleration of e-beam bunches at RF frequency is not possible with normal-cavity RF accelerators, and usually the accelerated electron beam bunches are produced in macropulses of few tens of microsecond duration, which are generated at a repetition rate of 10–1000 Hz.

These characteristics of RF accelerators are fit to drive FEL oscillators in the IR to UV range in which the bunches repetition frequency (equal or subharmonic of the accelerator RF frequency) is synchronized with the round-trip circulation frequency of the radiation pulses in the FEL resonator (see **Figure 14**).

The FEL small signal gain, must be large enough to build-up the radiation field in the resonator from noise to saturation well within the macropulse duration.

RF-Linacs are essential facilities in synchrotron radiation centers, used to inject electron beam current into the synchrotron storage ring accelerator from time to time. Because of this reason, many FELs based on RF-LINACs were developed in synchrotron centers, and provide additional coherent radiation sources to the synchrotron radiation center users.

Figure 15 displays FELIX – a RF-LINAC FEL which is located in one of the most active FEL radiation user-centers in FOM – Holland.

Storage rings

Storage rings are circular accelerators in which a number of electron (or positron) beam bunches (typically of 50–500 pS pulse duration and hundreds of ampere peak current) are circulated continuously by means of a lattice of bending magnets and quadrupole lenses. Typical energies of storage ring accelerators are in the hundreds of MeV to GeVs range. As the electrons pass through the bending magnets, they lose a small amount of their energy due to emission of synchrotron radiation. This energy is replenished by a small RF acceleration cavity placed in one section of the ring. The electron beam bunch dimensions, energy spread, and emittance parameters are set in steady state by a balance between the electrons oscillations within the ring lattice and radiation damping due to the random synchrotron emission process. This produces high-quality (small emittance and energy spread) continuous train of electron beam bunches, that can be used to drive a FEL oscillator placed as an insertion device in one of the straight sections of the ring between two bending magnets.

Demonstrations of FEL oscillators, operating in a storage ring, were first reported by the French (LURE-Orsay) in 1987 (at visible wavelengths) and the Russians (VEPP-Novosibirsk) in 1988 (in the ultra-violet). The short wavelength operation of storage-ring FELs is facilitated by the high energy, low emittance and low energy spread parameters of the beam.

Since storage ring accelerators are at the heart of all synchrotron radiation centers, one could expect that FEL would be abundant in such facilities as insertion devices. There is, however, a problem of interference of the FEL operating as an insertion device in the normal operation of the ring itself. The energy spread increase, induced in the electron beam during the interaction in a saturated FEL oscillator, cannot be controlled by the synchrotron radiation damping process, if the FEL operating power is too high.

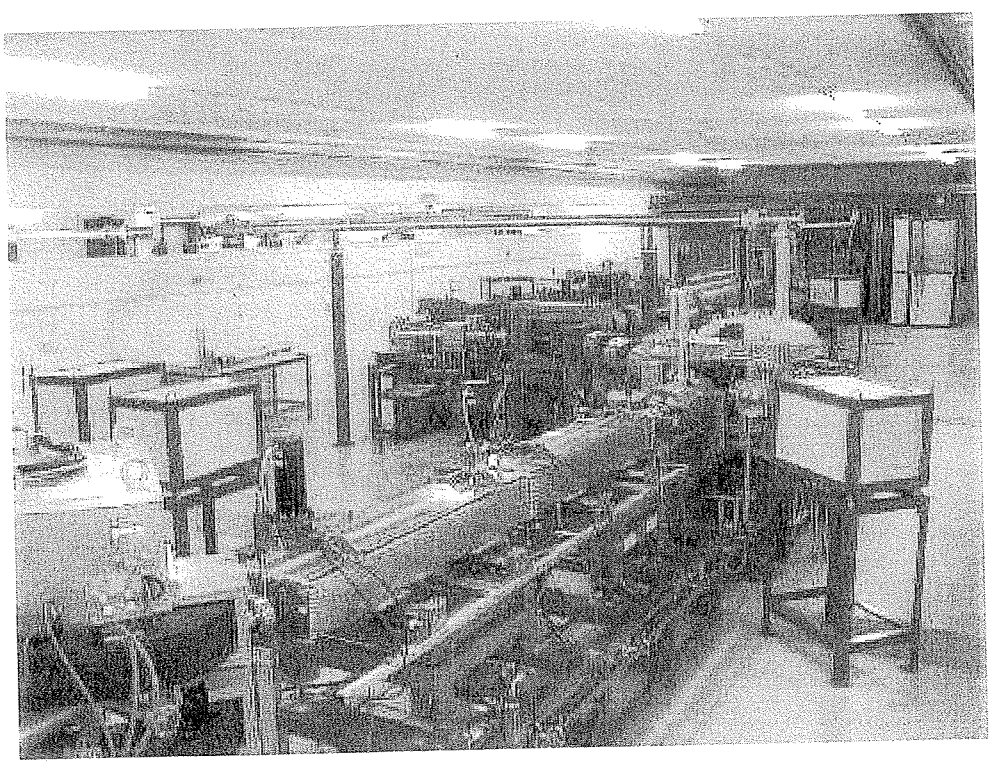

Figure 15 The FELIX RF-Linac FEL operating as a radiation users center in F.O.M. Netherlands. (Courtesy of L. van der Meer, F.O.M.)

This limits the FEL power to be kept as a fraction of the synchrotron radiation power dissipation all around the ring (the 'Renieri Limit'). The effect of the FEL on the e-beam quality, reduces the lifetime of the electrons in the storage ring, and so distrupts the normal operation of the ring in a synchrotron radiation user facility.

To avoid the interference problems, it is most desirable to operate FELs in a dedicated storage ring. This also provides the option to leave long enough straight sections in which long enough wigglers provide sufficient gain for FEL oscillation. **Figure 16** displays the Duke storage ring FEL, which is used as a unique radiation user facility, providing intense coherent short wavelength radiation for applications in medicine, biology, material studies, etc.

Superconducting (SC) RF-LINACS

When the RF cavities of the accelerator are superconducting, there are very low RF power losses on the cavity walls, and it is possible to maintain continuous acceleration field in the RF accelerator with a moderate-power continuous RF source, which delivers all of its power to the electron beam kinetic energy. Combining the SC-RF-LINAC technology with an FEL oscillator, pioneered primarily by Stanford University and Thomas Jefferson Lab (TJL) in the US and JAERI Lab in Japan, gave rise to an important scheme of operating such a system in a current recirculating energy retrieval mode. This scheme revolutionized the development of FELs in the direction of high-power, high-efficiency operation, which is highly desirable, primarily for industrial applications (material processing, photochemical production, etc.).

In the recirculating SC-RF-LINAC FEL scheme the wasted beam emerging out of the wiggler after losing a fraction of only few percents (see eqn [89]) out of its kinetic energy, is not dumped into a beam-dump, as in normal cavity RF accelerators, but is re-injected, after circulation, into the SC-RF accelerator. The timing of the wasted electron bunches re-injection is such that they experience a deceleration phase along the entire length of the accelerating cavities. Usually, they are re-injected at the same cell with a fresh new electron bunch injected at an acceleration phase, and thus the accelerated fresh bunch receives its acceleration kinetic energy directly from the wasted beam bunch, that is at the same time decelerated. The decelerated wasted beam bunches are then dumped in the electron beam dump at much lower energy than without recirculation, at energies that are limited primarily just by the energy spread induced in the beam in the FEL laser-saturation process. This scheme, not only increases many folds the over-all energy transformation efficiency from wall-plug to radiation, but would solve significant heat dissipation and radioactivity activation problems in a high-power FEL design.

Figure 17 displays the TJL Infrared SC-RF-LINAC FEL oscillator, that demonstrated for the first time

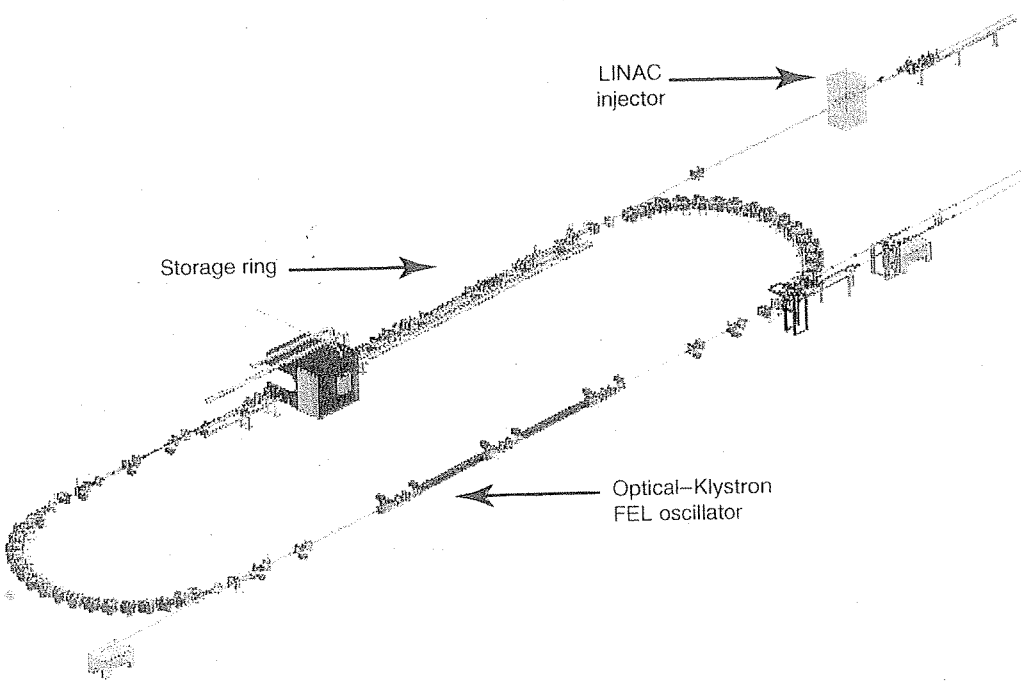

Figure 16 The Duke – University Storage Ring FEL operating as a radiation-users center in N. Carolina, USA. (Rendering: Matthew Busch, courtesy of Glenn Edwards, Duke FEL Lab.)

record high average power levels – nearly 10 kWatt at optical frequencies (1–14 μm). The facility is in upgrade development stages towards eventual operation at 100 kWatt in the IR and 1 kWatt in the UV. It operates in the framework of a laser material processing consortium and demonstrates important material processing applications, such as high-rate micromachining of hard materials (ceramics) with picoSecond laser pulses.

The e-beam current recirculation scheme of SC-RF-LINAC FEL has a significant advantage over the e-beam recirculation in a storage ring. As in electrostatic accelerators, the electrons entering the wiggler are 'fresh' cold-beam electrons from the injector, and not a wasted beam corrupted by the laser saturation process in a previous circulation through the FEL. This also makes it possible to sustain high average circulating current despite the disruptive effect of the FEL on the e-beam. This technological development has given rise to a new concept for a radiation-user facility light-source 4GLS (fourth-generation light source), which is presently in a pilot project development stage at Daresbury Lab in the UK (see **Figure 18**). In such a scheme, IR and UV FEL oscillators and XUV SASE-FEL can be operated together with synchrotron magnet dipole and wiggler insertion devices without disruptive interference. Such a scheme, if further developed, can give rise to new radiation-user, light-source facilities, that can provide a wider range of radiation parameters than synchrotron centers of previous generation.

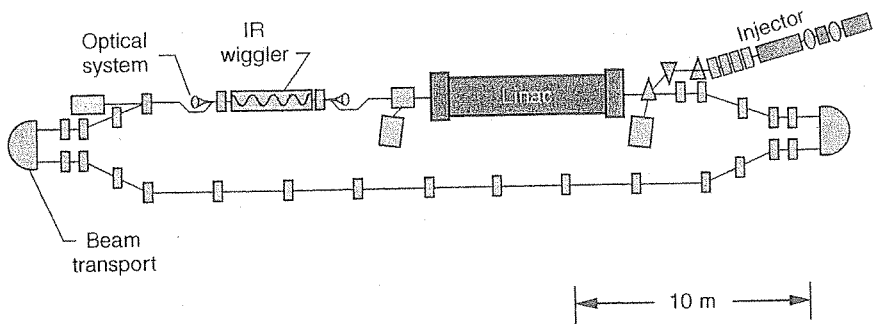

Figure 17 The Thomas Jefferson Lab. recirculating beam-current superconducting Linac FEL operating as a material processing FEL-user center in Virginia USA (Courtesy of S. Benson, Thomas Jefferson Laboratory).

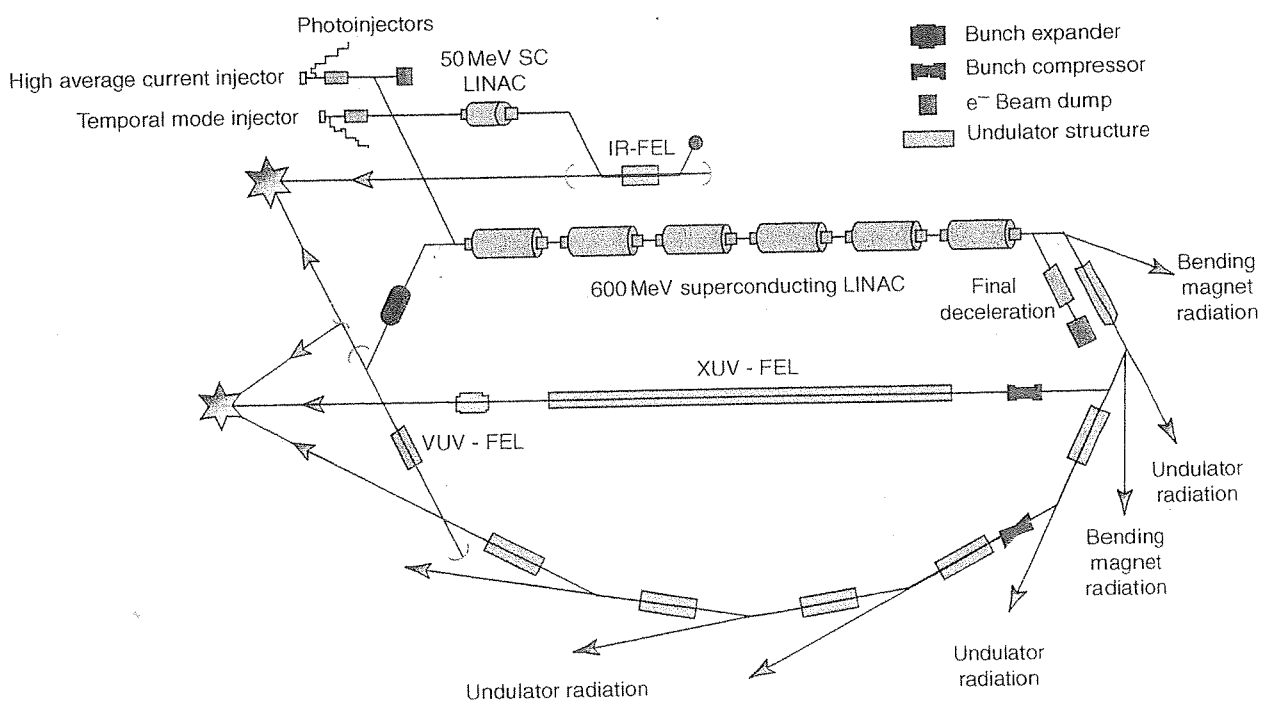

Figure 18 The Daresbury Fourth Generation Light-Source concept (4GLS). The circulating beam-current superconducting Linac includes SASE-FEL, bending magnets and wigglers as insertion devices. (Courtesy of M. Poole, Damesbury Laboratory)

Magnetic Wiggler Schemes

The optical klystron

The stimulated emission process in FEL (see Figure 7c) is based on velocity (energy) bunching of the e-beam in the first part of the wiggler, which turns into density bunching along the central part of the wiggler, and then the density-bunched electron beam performs 'negative work' on the radiation wave and emits radiative energy in the last part of the wiggler. In the OK, these steps are carried out in three separate parts of the wiggler: the energy bunching wiggler section, the dispersive magnet density buncher, and the radiating wiggler section (see Figure 7b).

A schematic of the OK is shown in Figure 19. The chicane magnetic structure in the dispersive section brings all electrons emerging from the bunching wiggler back onto the axis of the radiating wiggler, but provides variable delay $\Delta t_{di} = \int_{L_b}^{L_b+L_d} (v_{zi}^{-1} - v_{ph}^{-1})\, dz = [d(\Delta t_d)/d\gamma]\delta\gamma_i$ relative to the pondermotive wave phase to different electrons, which acquired different energy modulation increments $\delta\gamma_i = \gamma_i - \gamma_{ph}$ in the final section. The radiation condition is satisfied whenever the bunch-center phase satisfies $\Delta\varphi_d = \omega\Delta t_d = \pi/2 - 2m\pi$ (see Figure 7b). However, because the energy dispersion coefficient $d(\Delta t_d)/d\gamma$, is much larger in the chicane than in a wiggler of the same length, the density bunching amplitude, and consequently the OK gain, are much larger than in a uniform wiggler FEL of the same length.

The OK was invented by Vinokurov and Skrinsky in 1977 and first demonstrated in 1987 at visible wavelengths in the ACO storage ring of LURE in Orsay, France, and subsequently in 1988 at UV wavelengths, in the VEPP storage ring in Novosibirsk, Russia. The OK is an optimal FEL configuration, if used as an insertion device in a storage ring, because it can provide sufficient gain to exceed the high lasing threshold at the short operating wavelengths of a high-energy storage-ring FEL, and still conform with the rather short straight sections available for insertion devices in conventional synchrotron storage rings. It should be noted that the OK is equivalent to a long wiggler FEL of length L_{eff} of equal gain, and therefore its axial velocity spread acceptance is small (this is determined from the cold beam limit $\bar{\theta}_{th} \ll \pi$ with L_{eff} used in eqn [52]). This too is consistent with storage ring accelerators, which are characterized by small energy spread and emittance of the electron beam.

Radiation emission at harmonic frequencies

In a linear wiggler (eqn [2]), the axial velocity:

$$\beta_z = [\beta^2 - (a_w/\gamma)^2 \cos^2 k_w z]^{1/2} \qquad [92]$$

is not constant. It varies with spatial periodicity $\lambda_w/2$, and in addition to its average value $\bar{\beta}_z = [\beta^2 - a_w^2/2\gamma^2]^{1/2}$, contains Fourier components of spatial frequencies $2mk_w$ $(m = 1, 2, \ldots)$. When $a_w \gg 1$, the axial oscillation deforms the sinusoidal trajectory of the electrons in the wiggler (eqns [22] and [23]), and in a frame of reference moving at the average velocity $\bar{\beta}_z$, the electron trajectories in the wiggling $(x-z)$ plane forms an figure 8 shape, rather than a pure transverse linear motion. In the laboratory frame this leads to synchrotron undulator emission in the forward direction at all odd harmonic frequencies of ω_0, corresponding to substitution of $k_w \rightarrow (2m+1)k_w$ $(m = 1, 2, 3, \ldots)$ in eqn [6]:

$$\omega_{2m+1} = (2m+1)\omega_0 \cong 2\gamma_z^2 c(2m+1)k_w \qquad [93]$$

All the stimulated emission gain expressions, presented earlier for the fundamental harmonic, are valid with appropriate substitution of

$$\theta_{2m+1} = \frac{\omega}{v_z} - k_z - (2m+1)k_w \qquad [94]$$

instead of eqn [43], and substitution of the harmonic-weight Bessel-function coefficient of

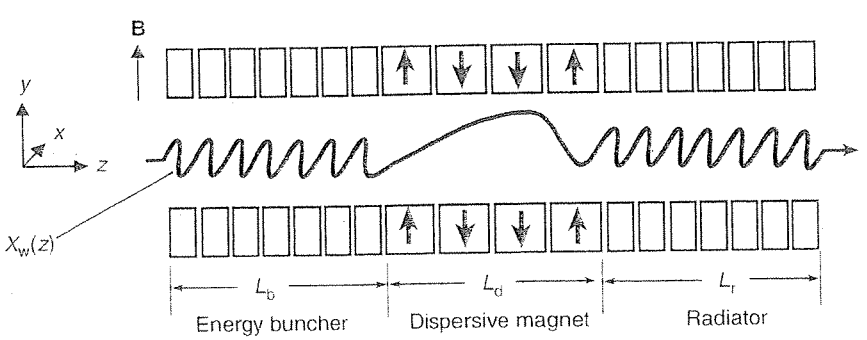

Figure 19 Schematics of the Optical–Klystron, including an energy bunching wiggler, a dispersive magnet bunching section and a radiating wiggler.

harmonic $2m+1$:

$$A_{JJ,2m+1} = \left\{ J_m\left[\frac{(2m+1)a_w^2}{2(a_w^2+2)}\right] - J_{m+1}\left[\frac{(2m+1)a_w^2}{2(a_w^2+2)}\right]\right\}(2m+1) \quad [95]$$

instead of A_{JJ} (eqn [39]) in eqns [38], [59] and [81]. These coefficients become significant for $m \neq 0$, only in the limit of relativistic transverse motion, $a_w > 1$. Note that in this limit, the fundamental harmonic coefficient becomes less than unity $A_{JJ} < 1$, and for operating at the fundamental harmonic, there is no benefit to increase the wiggler field.

FEL lasing at harmonic frequencies has been observed in several experiments. It provides a way to operate at higher frequencies when the available e-beam energy is limited. Enhanced coherent emission at odd harmonic frequencies takes place in a linear wiggler with $a_w > 1$, even if the FEL lases only at the fundamental frequency and the oscillation threshold at the higher harmonics is not exceeded. This can also be an undesirable effect in FEL oscillator realization. In several FEL oscillator experiments, emission of harmonic frequencies in the deep UV caused degradation damage to the optical mirrors of the resonator, creating an engineering problem of keeping a reasonable operating lifetime of the laser.

Electromagnetic pump (Compton scattering)

The magnetic wiggler field in eqns [2] or [3] can be replaced with the electromagnetic field of an intense coherent radiation beam propagating in counter direction to the electron beam:

$$[\mathbf{E}_w(\mathbf{r},t), \mathbf{B}_w(\mathbf{r},t)] = \mathrm{Re}\left\{[\tilde{E}_w, \tilde{B}_w]e^{-i\omega_w t - ik_{zw} z}\right\} \quad [96]$$

The pondermotive wave, resulting from the nonlinear beat of the signal wave (eqn [26]) and 'wiggler' (pump) (eqn [96]) has frequency $\omega - \omega_w$ and wavenumber $k_s + k_w$. The FEL formulation remains valid for this case with corresponding modifications. In particular, the detuning parameter becomes:

$$\theta = \frac{\omega - \omega_w}{v_z} - k_z - k_w \quad [97]$$

and the synchronism radiation condition (corresponding to $\theta = 0$) is in the free space propagation limit ($k_z = \omega/c$, $k_{zw} = \omega_w/c$):

$$\omega = \frac{1+\beta_z}{1-\beta_z}\omega_w = (1+\beta_z)^2\gamma_z^2\omega_w \cong 4\gamma_z^2\omega_w \quad [98]$$

The last part of the equality is valid only for the highly relativistic limit $\gamma_z \gg 1$.

This observation sheds a different light on the FEL device, which can be viewed (see **Figure 3**) as a parametric process involving stimulated scattering of the pump (wiggler) wave off the electron beam, that acts as the nonlinear medium, amplifying the signal wave. The process can therefore be viewed as 'stimulated Compton scattering', and in the collective regime, where a third wave (plasma- space-charge wave) is excited – stimulated Raman scattering Furthermore, it was shown that the system satisfies the 'Manley–Rowe' relations, namely in a quantized model, a pump photon is absorbed for each signal wave photon generated (in the Raman regime – also a plasmon is generated).

The electromagnetic pump scheme seems an attractive option for realizing high-frequency FELs with a moderate energy electron beam. Whether a high-power mm-wave tube or a high-intensity laser are considered as the source of the electromagnetic pump, the 'wiggler' period would be much shorter than attainable with a magnetic wiggler, and there is an additional factor X2 in the radiation frequency expression in eqn [98] relative to eqn [6]. Nevertheless, such FELs have not been realized, because the intensity or beam pulse duration of available sources are not sufficient to attain sufficient gain or oscillation build-up time for an FEL amplifier or an FEL oscillator respectively. A natural electromagnetic pump can be the intense signal radiation generated by the FEL itself in a conventional FEL, which is reflected back to interact again with the electron beam, with which it is naturally synchronized. Few experiments have been carried out to demonstrate that such a two-stage FEL concept is possible.

While stimulated emission gain is hard to attain in these schemes, spontaneous emission (Doppler shifted Compton scattering off the beam) is always possible. Indeed, such schemes provide quite unique sources of picoSecond-pulsed X-ray to gamma-ray radiation, which are provided to users in several FEL user-facilities, such as Vanderbilt University and Duke University.

Tapered wiggler

When an electron beam, amplifying a radiation wave in an FEL, enters saturation, it loses axial kinetic energy in favor of the radiation field. While streaming in the axial direction it slows down relative to the pondermotive wave and stops interacting with it because it gets out of synchronism (eqn [29]) (or eqn [91]). It is possible to keep extracting more energy from the beam, if the PM wave phase velocity tapers down too, and continues to keep in

synchronism with the beam. Slowing down the PM wave can be done by the gradual increase of the wiggler wavenumber $k_w(z)$ (or decrease of its period $\lambda_w(z)$), so that eqns [29] or [91] keep being satisfied for a given frequency, even if v_z (or γ_z) goes down.

A more correct description of the nonlinear interaction dynamics of the electron beam in a saturated tapered-wiggler FEL is depicted in Figure 20: the electron trap synchronism energy $\gamma_{ph}(z)$ tapers down (by design) along the wiggler, while the trapped electrons are forced to slow down with it, releasing their excess energy by enhanced radiation. An upper limit estimate for the extraction efficiency of such a tapered wiggler FEL would be:

$$\eta_{ext} = \frac{\gamma_{ph}(0) - \gamma_{ph}(L)}{\gamma_{ph}(0)} \qquad [99]$$

and the corresponding radiative power generation would be: $\Delta P = \eta_{ext} I_b E_k / e$. In practice, the phase-space area of the tapered wiggler separatrix is reduced due to the tapering, and only a fraction of the electron beam can be trapped, which reduces correspondingly the practical enhancement in radiative extraction efficiency and power.

An alternative wiggler tapering scheme consists of tapering the wiggler field $B_w(z)$ (or wiggler parameter amplitude $a_w(z)$). If these are tapered down, the axial velocity and axial energy (eqn [7]) can still keep constant (and in synchronism with the PM wave) even if the beam energy γ goes down. Thus, in this scheme, the excess radiative energy extracted from the beam comes out of its transverse (wiggling) energy.

Efficiency and power enhancement of FEL by wiggler tapering have been demonstrated experimentally both in FEL amplifiers (first by Livermore, 1985) and oscillators (first by Los-Alamos, 1983). This elegant way to extract more power from the beam still has some limitations. It can operate efficiently only at a specified high radiation power level for which the tapering was designed. In an oscillator, a long enough untapered section must be left to permit sufficient small signal gain in the early stages of the laser oscillation build-up process.

FEL Oscillators

Most FEL devices are oscillators. As in any laser, in order to turn the FEL amplification process into an oscillation process, one provides a feedback mechanism by means of an optical resonator. In steady state saturation, $GR_{rt} = 1$, where R_{rt} is the round trip reflectivity factor of the resonator and $G = P(L)/P(0)$ is the saturated single-path gain coefficient of the FEL. To attain oscillation, the small signal (unsaturated) gain, usually given by the small gain expression in eqn [53], must satisfy the lasing threshold condition $G > 1/R_{rt}$, as in any laser.

When steady state oscillation is attained, the oscillator output power is:

$$P_{out} = \frac{T}{1 - R_{rt}} \Delta P_{ext} \qquad [100]$$

where $\Delta P_{ext} = \eta_{ext} I_0 (\gamma_0 - 1) mc^2/e$ and η_{ext} is the extraction efficiency, usually given by eqn [89] (low-gain limit).

Usually, FEL oscillators operate in the low-gain regime, in which case $1 - R_{rt} = L + T \ll 1$ (where L is the resonator internal loss factor). Consequently, then $P_{out} \cong \Delta P_{ext} T/(L + T)$, which would give a maximum value, depending on the saturation level of the oscillator. In the general case, one must solve the nonlinear force equations together with the resonator feedback relations of the oscillating radiation mode, in order to maximize the output power (eqn [100]) or efficiency by choice of optimal T for given L.

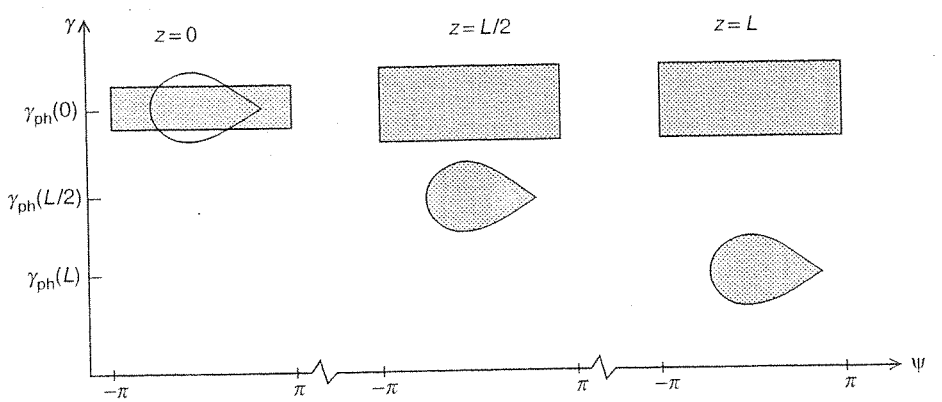

Figure 20 'Snapshots' of the trap at three locations along a tapered wiggler FEL.

In an FEL oscillator operating with periodic electron bunches (as in RF-acclerator based FEL), the solution for the FEL gain and saturation dynamics requires extension of the single frequency solution of the electron and electromagnetic field equations to the time domain. In principle, the situation is similar to that of a mode-locked laser, and the steady state laser pulse train waveform constitutes a superposition of the resonator longitudinal modes that produces a self-similar pulse shape with the highest gain (best overlap with the e-beam bunch along the interaction length). Because the e-beam velocity v_{z0} is always smaller (in an open resonator) than the group velocity of the circulating radiation wavepacket, the radiation wavepacket slips ahead of the electron bunch one optical period λ in each wiggling period (Slippage effect). This reduces the overlap between the radiation pulse and the e-beam bunch along the wiggler (see **Figure 14**) and consequently decreases the gain. Fine adjustment of the resonator mirrors (as shown in **Figure 14**) is needed to attain maximal power and optimal radiation pulse shape. The pulse-slippage gain reduction effect is negligible only if the bunch length is much longer than the slippage length $N_w\lambda$, which can be expressed as:

$$\tau_p \gg 2\pi/\Delta\omega_L \qquad [101]$$

where $\Delta\omega_L$ is the synchrotron undulator radiation frequency bandwidth (eqn [55]). This condition is usually not satisfied in RF-accelerator FELs operating in the IR or lower frequencies, and the

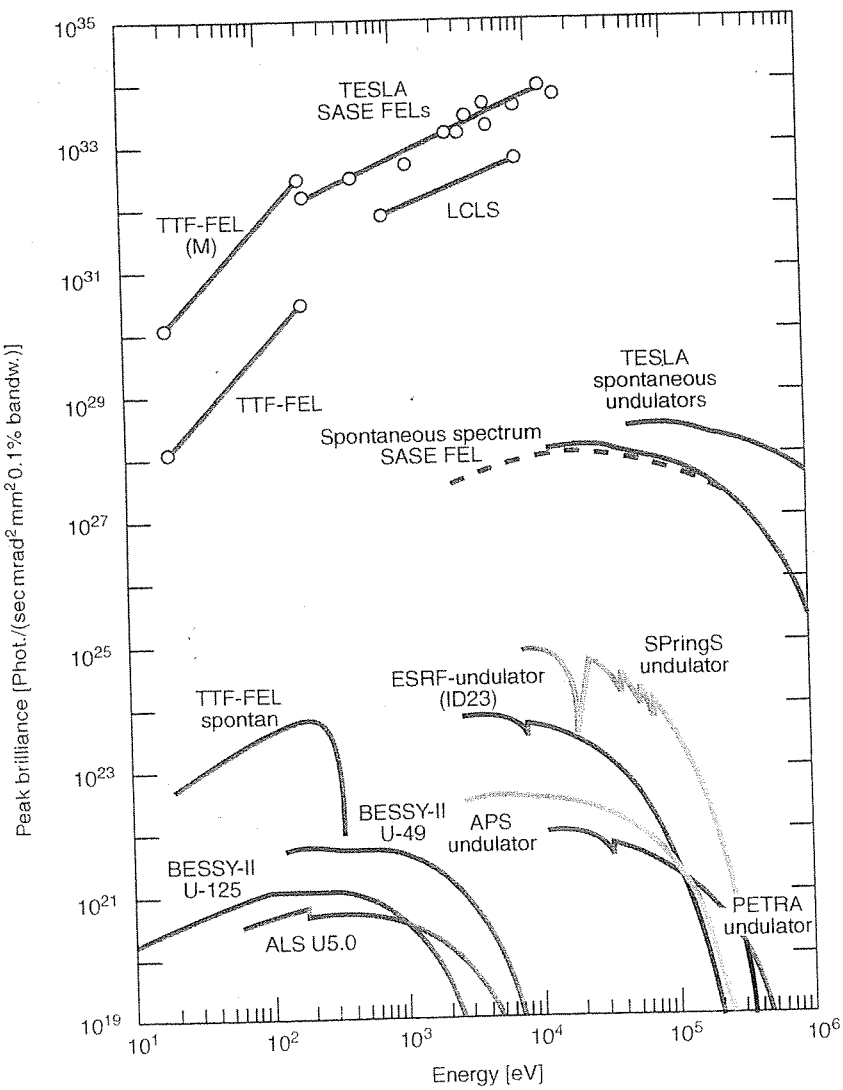

Figure 21 Anticipated peak brightness of SASE FELs (TTF-DESY, LCLS-SLAC) in comparison to the undulators in present third generation Synchrotron Radiation sources. Figure courtesy of DESY, Hamburg, Germany.

slippage effect gain reduction must be then taken into account.

An FEL operating in the cold-beam regime constitutes an 'homogeneous broadening' gain medium in the sense of conventional laser theory. Consequently, the longitudinal mode competition process that would develop in a CW FEL oscillator, leads to single-mode operation and high spectral purity (temporal coherence) of the laser radiation. The minimal (intrinsic) laser linewidth would be determined by an expression analogous to the Schawlow–Towns limit of atomic laser:

$$(\Delta f)_{\text{int}} = \frac{(\Delta f_{1/2})^2}{I_b/e} \qquad [102]$$

where $\Delta f_{1/2}$ is the spectral width of the cold resonator mode. Expression [102] predicts extremely narrow linewidth. In practice, CW operation of FEL was not yet attained, but Fourier transform limited linewidths in the range of $\Delta f/f_0 \cong 10^{-6}$ were measured in long-pulse electrostatic accelerator FELs. In an FEL oscillator, based on a train of e-beam bunches (e.g., an R.F. accelerator beam), the linewidth is very wide and is equal to the entire gain bandwidth (eqn [56]) in the slippage dominated limit, and to the Fourier transform limit $\Delta\omega \cong 2\pi/\tau_p$ in the opposite negligible-slippage limit (eqn [101]). Despite this slippage, it was observed in RF-LINAC FEL that the radiation pulses emitted by the FEL oscillator are phase corrected with each other, and therefore their total temporal coherence length may be as long as the

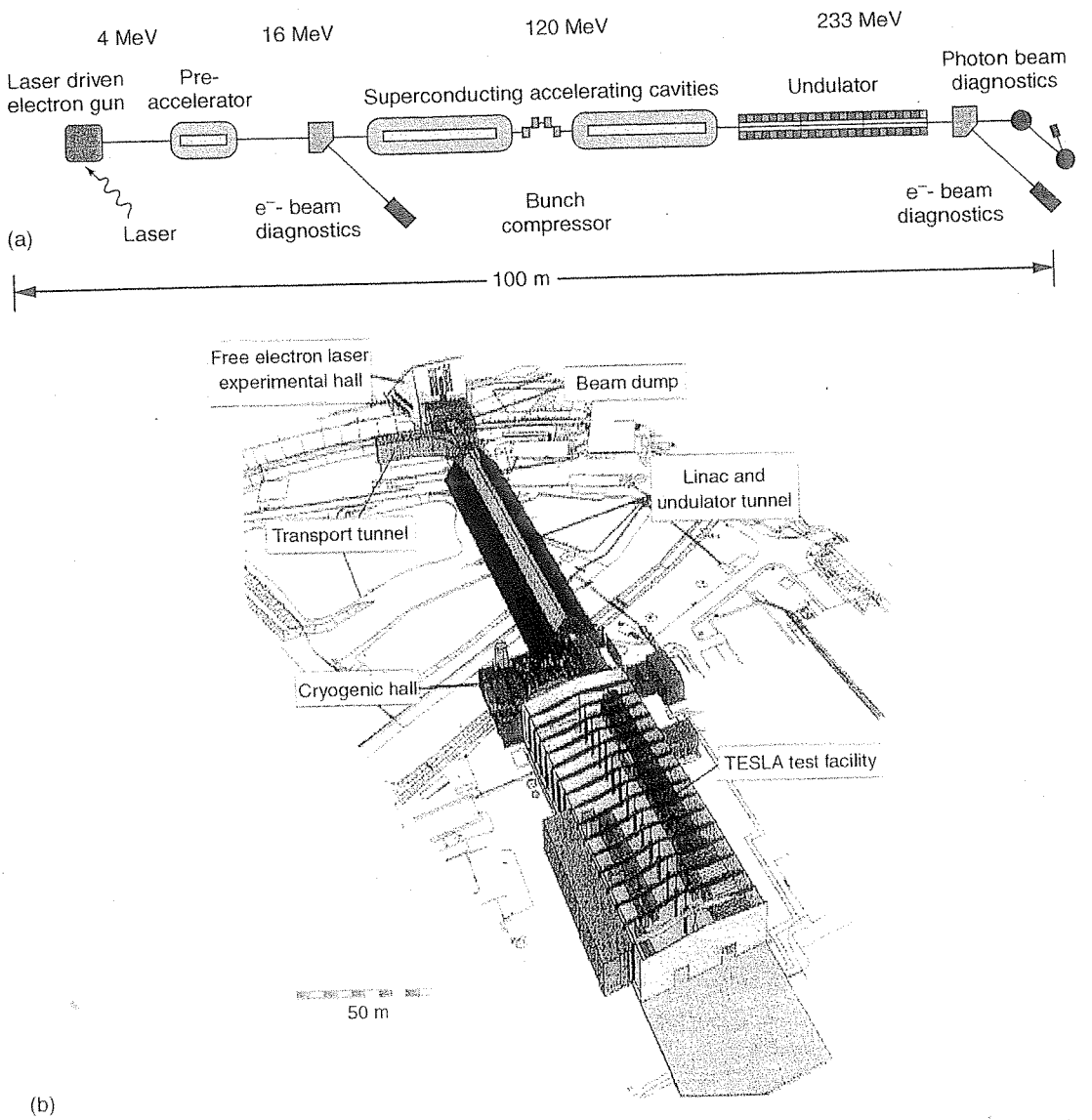

Figure 22 Phase 1 of the SASE FE L (TTF VUV-FEL1): (a) Accelerator layout scheme; (b) General view of the TESLA test facility. Figure courtesy of DESY, Hamburg, Germany.

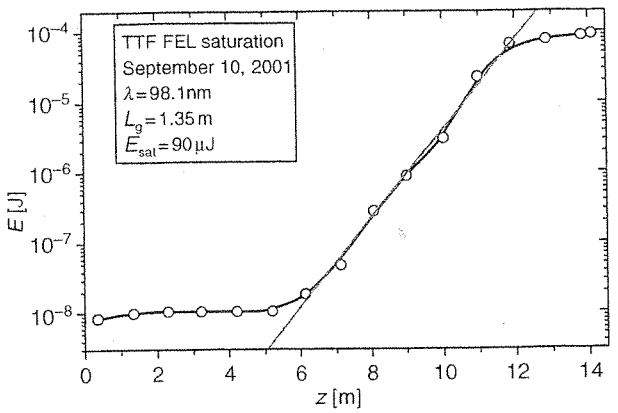

Figure 23 Measured SASE radiation pulse energy versus wiggler length from small signal regime up to saturation. Figure courtesy of DESY, Hamburg, Germany.

entire e-beam macropulse duration, and in this sense the continuously pulsed oscillator radiation output is also very coherent.

SASE FEL

This kind of FEL is of high interest and importance, because of its ability to operate at very short wavelengths, up to the VUV and X-rays, where lasers are hard to construct. **Figure 21** illustrates the significant advantage of SASE-FEL over conventional synchrotron radiation sources in terms of the spectral brightness parameter. SASE-FEL sources promise both peak and average brightness parameters, at least five orders of magnitude higher than synchrotron sources. There are expectations that such new sources of femptoSecond pulsed bright X-ray radiation will be an important tool for studies in physics, biology, and chemistry in regimes not accessible so far, such as a single bio-cell imaging.

An impressive research and development work, carried out in the last decade, in American (UCLA, Brookhaven NSLS, Argone) and German (Desy–Tesla Test Facility – TTF), has led the road to understanding and implementation of the SASE concept in the optical frequency regime up to the VUV, demonstrating very high peak powers (up to saturation) and brightness. Record short wavelength $\lambda = 80$ nm was achieved at TTF in 2001. A number of ambitious projects (LCLS in SLAC – US, TESLA-X-FEL in DESY – Germany) are in the development stage, having the goal to achieve lasing near $\lambda = 1$ Å with exceptional optical beam characteristics.

VUV to X-ray SASE FELs are, of course, very large devices, requiring a long high-energy LINAC accelerator and a long wiggler. **Figure 22** displays the TTFVUV FEL, which is based on a GeV Superconducting RF-LINAC and a 13.5 m long wiggler. The future TESLA X-ray FEL will employ a 27 m long wriggler.

The SASE FEL is only partially temporally coherent (its spectral linewidth is quite wide – eqn [64]). It is still very bright due to its high power and its very high spatial coherence. The high (diffraction limited) spatial coherence is due to the effect of optical-guiding over the electron beam. Such guiding is facilitated by the positive real part of the interaction-modified wavenumber of the wave δk_1 (eqn [60]). This creates an effective higher index of refraction inside the electron beam, which provides optical guiding similarly to an optical fiber.

Figure 23 displays experimental data of SASE power measurement versus wiggler length. It confirms the exponential growth rate up to the saturation level predicted by theory. The pulse-energy data points in the curve are the results of averaging over many pulses. It should be noted that there is always wide scattering of power intensities from shot to shot, which is inherent in the device (due to the statistical fluctuations of the electron beam current) until saturation is attained.

Various new schemes are being investigated to further improve the optical properties of SASE-FEL. For example, optical filtering of the synchrotron undulator radition after a short section in the beginning of the wiggler, may be a way to narrow down the frequency linewidth of the SASE FEL. Since the development of this device is still in its infancy, it can be predicted with high certainty that this kind of light source technology will reach a 'bright' future.

Further Reading

Benson SV (2003) Free electron lasers push into new frontiers. *Optics and Photonic News* 14: 20–25.

Brau CA (1990) *Free Electron Lasers*. New York: Academic Press.

Colson WB, Pellegrini C and Renieri A (1990) *Laser Handbook*, vol. 6. North Holland.

Freund HP and Antonsen TM Jr (1992) *Principles of Free Electron Lasers*. Chapman & Hall.

Friedman A, Gover A, Ruschin S, Kurizki G and Yariv A (1988) Spontaneous and stimulated emission from quasi-free electrons. *Reviews of Modern Physics* 60: 471–535.

Saldin EL, Schneidmiller EA and Yurkov MV (1999) *The Physics of Free Electron Lasers*. Springer.

The World Wide Web Virtual Library – Free Electron Laser research and applications, http://sbfel3.ucsb.edu/www/fel_table.html